

MATHEMATISCHES FORSCHUNGSINSTITUT OBERWOLFACH

Report No. 39/2016

DOI: 10.4171/OWR/2016/39

Multiscale Interactions in Geophysical Fluids

Organised by
Rupert Klein, Berlin
Shafer Smith, New York
Jacques Vanneste, Edinburgh

14 August – 20 August 2016

ABSTRACT. The dynamics of the atmosphere and ocean involves a broad range of spatial and temporal scales, many of which emerge through complex nonlinear mechanisms from forcings at very different scales. This poses major challenges for the numerical prediction of the weather, ocean state and climate: many processes have scales that are too small to be resolved yet they play an essential role in determining large-scale features. This workshop examined how modern mathematical methods – ranging from multiscale asymptotics to adaptive numerical methods and stochastic modelling – can be applied to represent the large-scale impact of these small-scale processes and improve both deterministic and probabilistic predictions.

Mathematics Subject Classification (2010): 86A10, 37N10, 76U05.

Introduction by the Organisers

One of the most striking features of the dynamics of both the atmosphere and the ocean is the crucial role played by a range of small-scale, high-frequency phenomena in determining the large-scale flow. Examples of this abound, from the role of gravity waves on the middle-atmospheric circulation and the driving of jets by turbulent motion, to the impact of small-scale mixing on the deep ocean. This poses major challenges for atmospheric and oceanic predictions, of course, since these are based on numerical models that necessarily have limited spatial and temporal resolutions.

Advanced mathematical methods have an important part to play in addressing these challenges: a range of mathematical techniques, including multiscale asymptotics, adaptive numerics, dimensionality reduction, and stochastic and data-driven models, can be brought to bear on the problems. Their effective use depends on close interactions between mathematicians and atmosphere and ocean scientists. The workshop aimed at stimulating these interactions, by bringing together researchers from across applied mathematics and geophysical fluid dynamics to discuss key mathematical challenges arising from recent developments in atmosphere and ocean dynamics. It was well attended, with 45 participants from 10 countries representing weather centres as well as universities.

The workshop was structured around 7 thematic sessions, each consisting of 3 lectures that combined review material with descriptions of recent results. The first session highlighted the complexity of geophysical flows, with lectures by Nikurashin on the impact of small-scale topography on ocean flow, by Pauluis on the effect of moisture on the meridional circulation of the atmosphere, and by Muller on the self-organisation of atmospheric convection. Sessions 2 and 3 were dedicated to a range of multiscale methods applied to internal waves in the atmosphere (Achatz) and in the ocean (Young), to convection in planetary atmospheres (Julien), to the Julian–Madden oscillation (Stechmann), and to stochastic parameterisations (Gottwald, Grooms). Session 4 discussed rigorous results, with Doering on enstrophy dissipation, Bresch on the compressible Navier–Stokes equations, and Titi on data assimilation. Numerical methods are of course key to much of atmosphere and ocean modelling. They were represented at the workshop in session 5, with Korn and Smolakiewicz’s lectures on state-of-the art numerical models based on unstructured grids, and Wingate’s lecture on methods that best exploit distributed computer architectures. Session 6 centred on data-driven modelling, with discussions of systematic approaches to the classification of multi-scale time series with inherent non-stationarity due to latent or unobserved scales and variables (Horenko), of stochastic parameterizations of sub-gridscale turbulence motivated by high-resolution simulations (Zanna), and of turbulent fluctuations in stably stratified boundary layers (Vercauteren). Probabilistic techniques are increasingly applied to geophysical fluids. This was reflected in the last lecture session with contributions by Bouchet on large-deviation techniques, by Kuksin on weak turbulence, and by Holm on variational stochastic models.

All the lectures involved a good degree of audience participation, with questions and clarifications making it possible to fully engage the multidisciplinary audience. They were complemented by a successful poster session, which gave the opportunity to ten researchers to present their recent results, and by many informal discussions. The workshop enabled participants to share ideas and work collaboratively on what emerged as the most promising avenues for the applications of modern mathematical methods to geophysical fluid dynamics.

The organizers would like to thank the MFO staff for their outstanding support prior to and during the meeting.

Acknowledgement: The MFO and the workshop organizers would like to thank the National Science Foundation for supporting the participation of junior researchers in the workshop by the grant DMS-1049268, “US Junior Oberwolfach Fellows”.

Workshop: Multiscale Interactions in Geophysical Fluids**Table of Contents**

Maxim Nikurashin	
<i>Routes to unbalanced motions at rough topography in the Southern Ocean</i>	2231
Olivier Pauluis (joint with Olivier Pauluis)	
<i>Meridional circulation on moist isentropes</i>	2233
Caroline Muller (joint with Sandrine Bony)	
<i>Self-Aggregation of atmospheric convection in idealized simulations</i>	2234
Ulrich Achatz	
<i>Mesoscale and Sub-Mesoscale Wave Dynamics Throughout all Atmospheric Layers</i>	2236
William R. Young (joint with Gregory L. Wagner and Gwenaël Ferrando)	
<i>Scattering of the Internal Tide by Balanced Flow</i>	2238
Keith Julien	
<i>Multiscale Methods in Strongly Anisotropic Geophysical Systems</i>	2240
Samuel N. Stechmann	
<i>Multiscale asymptotics for the Madden-Julian oscillation and tropical-extratropical interactions</i>	2242
Georg A. Gottwald (joint with Jeroen Wouters)	
<i>Beyond the limit of infinite time-scale separation: Edgeworth approximations and homogenisation</i>	2243
Ian Grooms	
<i>A Gaussian-product stochastic Gent-McWilliams parameterization</i>	2244
Charles Doering	
<i>Applications of optimization and optimal control to some fundamental problems in mathematical fluid dynamics</i>	2246
Didier Bresch	
<i>Compressible Navier-Stokes Equations with Density Dependent Viscosities</i>	2247
Edriss Titi	
<i>Data assimilation algorithm for viscous geophysical models</i>	2250
Peter Korn	
<i>Numerical Methods for ocean General Circulation Models on Unstructured Grids</i>	2251

Beth A. Wingate (joint with Adam Peddle, Terry Haut)	
<i>The role of near-resonance in time-parallel numerical methods</i>	2252
Piotr K. Smolarkiewicz (joint with Joanna Szmelter, Feng Xiao)	
<i>Simulating all-scale atmospheric dynamics on unstructured meshes</i>	2254
Illia Horenko	
<i>Causality or correlation? Challenges in data-driven modeling of multiscale geophysical systems</i>	2257
Laure Zanna (joint with Luca Porta Mana, James Anstey, Tomos David, Thomas Bolton)	
<i>A Parametrization of Eddy-Mean Flow Interaction based on a Rivlin-Ericksen Stress Tensor</i>	2257
Nikki Vercauteren (joint with Larry Mahrt, Rupert Klein)	
<i>Different regimes of interactions between scales of motion in the stably stratified atmospheric boundary layer</i>	2259
Freddy Bouchet	
<i>Large deviations in climate dynamics: the examples of abrupt climate changes and extreme heat waves</i>	2260
Sergei B. Kuksin	
<i>The Zakharov-L'vov stochastic model for the wave turbulence</i>	2261
Darryl Holm	
<i>Variational principles for Stochastic fluid dynamics</i>	2264

Abstracts

Routes to unbalanced motions at rough topography in the Southern Ocean

MAXIM NIKURASHIN

The ocean circulation is forced at large, $O(100)$ km, scales primarily by winds at the surface and dissipated at small, $O(1)$ cm, scales by molecular viscosity in the turbulent boundary layers and ocean interior [5, 6]. The wind power input into the ocean is dominated by the Southern Hemisphere westerly winds aligned with the Antarctic Circumpolar Current (ACC) in the Southern Ocean [7]. The ACC is unstable to baroclinic instability which efficiently converts wind energy into mesoscale eddies. While mesoscale eddies dominate global kinetic energy of the ocean [6], the mechanisms of the transfer of their energy further down to the dissipation scale and the distribution of the energy dissipation in the ocean remain poorly understood.

Mesoscale eddies are nearly geostrophic and thus are characterised by inverse energy cascade, i.e. they tend to transfer energy toward larger scales [8]. A number of processes have been proposed to explain the transfer of the mesoscale eddy energy to smaller-scale unbalanced motions which then can take the energy down to the dissipation scales. Ocean western boundaries have been shown to be sites of elevated eddy-energy loss [10], where eddies generate internal Kelvin waves and hydraulically controlled motions [9]. In the Southern Ocean, where lateral boundaries are absent, geostrophic eddies have been suggested to dissipate primarily through interaction with the bottom boundary. Dissipation in the turbulent bottom boundary layer is believed to be a significant energy sink for oceanic flows including mesoscale eddies [11, 12]. Flows over rough small-scale topography can generate internal gravity waves that radiate energy away from topography into the ocean interior [13, 14]. Near the surface, frontal and mixed layer instabilities generate submesoscale eddies and have been suggested as possible routes for mesoscale eddy-energy dissipation [15, 16]. While these processes can extract energy from geostrophic flows, their efficiency and contribution to eddy energy dissipation and turbulence and mixing in the ocean interior are largely unclear.

In this study, realistic internal wave-permitting simulations of one of the hot spots of eddy activity in the Southern Ocean, the Macquarie Ridge region, are used to investigate the energy dissipation of the ACC fronts and eddies. The simulations are initialized and forced at open boundaries by the outputs from the Southern Ocean State Estimation (SOSE) and carried out for several years for a range of resolutions from the eddy-resolving, about 10 km, down to the submesoscale resolving and internal wave-permitting, about 800m, horizontal resolution. The total mechanical energy budget, including inflow and outflow of kinetic energy across the boundaries, surface wind power input and energy dissipation by bottom drag and interior viscous friction, is diagnosed and closed within a few percent of

the wind power input. The distribution of the viscous energy dissipation throughout the ocean and the relative contribution of the surface and deep ocean processes to the energy dissipation is quantified and discussed. The results show that the energy input is dominated by the wind work at the surface and the energy sink is dominated by the viscous friction acting on resolved small-scale motions in the flow. Bulk of the energy dissipation takes place in the deep ocean catalysed by rough small-scale topography.

Some fraction of the energy extracted from mesoscale eddies is radiated into the ocean interior in the form of internal waves, while the rest is dissipated close to topography. Energy radiated into the ocean interior can sustain turbulent mixing and hence impact global ocean circulation and climate. The linear theory used to estimate energy conversion into internal waves is formally valid in a limit of subcritical topography, or small topographic steepness parameter, i.e. when the characteristic topographic slope is smaller than the internal wave slope [e.g. 2, 3]. However, most of topography in the Southern Ocean varies from subcritical to critical, i.e. when the steepness parameter is of $O(1)$ and smaller [4]. In the limit of critical topography, when the linear theory is formally invalid, the predictions for the energy conversion into lee waves are corrected empirically based on the results from idealized two-dimensional (2D) numerical simulations [e.g. 13] and laboratory experiments [e.g. 1]. The idealized 2D simulations and laboratory experiments show that when the steepness parameter exceeds the critical value of 0.7 the energy conversion saturates. The saturation occurs because a certain fraction of the mean flow gets blocked by topography and thus does not lift isopycnals and generate internal waves.

To understand the partitioning between the radiating and non-radiating flow response to topography, in this study we test a hypothesis that 2D numerical simulations do not capture properly the finite amplitude topography effects on the generation of internal waves. In particular, the 2D simulations cannot represent the nonlinear flow splitting effect when the mean flow is split by a topographic obstacle and goes around rather than over it. The flow component going around an obstacle does not displace isopycnals in the vertical and hence does not generate internal gravity waves. We use a suite of 2D and three-dimensional (3D) numerical simulations to quantify the finite amplitude topography effects for realistic, multi-scale abyssal hill topography and flow characteristics observed in the Southern Ocean. The results show that the internal wave generation at the three-dimensional, finite bottom topography is suppressed compared to the two-dimensional case. The energy conversion saturates when the steepness parameter exceeds the critical value of 0.4, a value smaller than in 2D flows. The suppression is primarily associated with nonlinear flow splitting effect which reduces the amplitude of the internal waves radiated from topography and the associated wave breaking and turbulence away from topography.

In summary, the results of the realistic, high-resolution simulations of the Macquarie Ridge region of the Southern Ocean and simulations of turbulent flows at

rough topography show that rough small-scale bottom topography is very efficient at generation of small-scale motions and hence at the conversion of balanced mesoscale eddy energy to unbalanced internal waves and non-propagating motions near topography.

REFERENCES

- [1] Aguilar, D. and B. Sutherland Internal wave generation from rough topography *Phys. Fluids* **18**, 066603 (2006).
- [2] T. H. Bell Lee waves in stratified flows with simple harmonic time dependence *J. Fluid Mech.* **67**, 705–722 (1975).
- [3] T. H. Bell Topographically generated internal waves in the open ocean *J. Geophys. Res.* **80**, 320–327 (1975).
- [4] Nikurashin, M. & Ferrari, R. Global energy conversion rate from geostrophic flows into internal lee waves in the deep ocean. *Geophys. Res. Lett.* **38**, L08610 (2011).
- [5] Wunsch, C. & Ferrari, R. Vertical mixing, energy, and the general circulation of the oceans. *Ann. Rev. Fluid Mech.* **36**, 281–314 (2004).
- [6] Ferrari, R. & Wunsch, C. Ocean Circulation Kinetic Energy – Reservoirs, Sources and Sinks. *Ann. Rev. Fluid Mech.* **41**, 253–282 (2009).
- [7] Wunsch, C. The work done by the wind on the oceanic general circulation. *J. Phys. Oceanogr.* **28**, 2331–2339 (1998).
- [8] Charney, J. G. Geostrophic turbulence. *J. Atmos. Sci.* **28**, 1087–1095 (1971).
- [9] Hogg, A., Dewar, W., Berloff, P., & Ward, M. Kelvin wave hydraulic control induced by interactions between vortices and topography. *J. Fluid Mech.* **687**, 194–208 (2011).
- [10] Zhai, X., Johnson, H., & Marshall, D. Significant sink of ocean-eddy energy near western boundaries. *Nature Geoscience* **3**, 608–612 (2010).
- [11] Sen, A., Scott, R. B., & Arbic, B. K. Global energy dissipation rate of deep-ocean low-frequency flows by quadratic bottom boundary layer drag: Computations from current-meter data. *Geophys. Res. Lett.* **35**, L09606 (2008).
- [12] Arbic, B. K. et al. Estimates of bottom flows and bottom boundary layer dissipation of the oceanic general circulation from global high-resolution models. *J. Geophys. Res.* **114**, C02024 (2008).
- [13] Nikurashin, M. & Ferrari, R. Radiation and dissipation of internal waves generated by geostrophic flows impinging on small-scale topography: Theory. *J. Phys. Oceanogr.* **40**, 1055–1074 (2010).
- [14] Nikurashin, M. & Ferrari, R. Radiation and dissipation of internal waves generated by geostrophic flows impinging on small-scale topography: Application to the Southern Ocean. *J. Phys. Oceanogr.* **40**, 2025–2042 (2010).
- [15] Molemaker, M. J., McWilliams, J. C., & Capet, X. Balanced and unbalanced routes to dissipation in an equilibrated Eady flow. *J. Fluid Mech.* **654**, 35–63 (2010).
- [16] Ferrari, R. A Frontal Challenge for Climate Models. *Science* **332**, 316–317 (2011).

Meridional circulation on moist isentropes

OLIVIER PAULUIS

(joint work with Olivier Pauluis)

Isentropic analysis was originally introduced by [1] in the early development of dynamical meteorology. It relies on analyzing atmospheric motions on surface of constant potential temperature. In doing so, one takes advantage of the quasi-conservation of potential temperature to track parcel trajectories on time scales

longer than the eddy turnover. The equations of motion can be rewritten in isentropic coordinates [see e.g. 2], and used to diagnose the interactions between eddy and the mean meridional circulation.

Potential temperature is however not conserved in presence phase transition. This can be circumvented by using the equivalent potential temperature, which includes the effect of latent heat and is conserved for all reversible adiabatic motions, including phase transition. Recent studies [3, 4] have shown that the meridional circulation averaged on moist isentropes - defined as surfaces of constant equivalent potential temperature - differ substantially from the circulation on dry isentropes. In particular, the mass transport on moist isentropes is about twice as large in the midlatitudes than the mass transport on dry isentropes. This additional mass transport can be directly traced to the poleward flow of warm moist subtropical air that supplied energy and moisture to the midlatitudes stormtracks.

A mathematical challenge in using θ_e lies in that the topology of surface of constant θ_e is highly complex. In particular, the coordinate transformation from eulerian coordinates (x, y, z, t) to isentropic coordinates (x, y, θ_e, t) is often non-invertible due to the fact that the equivalent temperature profile in the atmosphere is often non-monotonic. In this talk, I introduce a weak formulation of the coordinate transformation, which makes it possible to express conservation laws in an arbitrary coordinate system. This formulation is applied to assess the mass and momentum transport in the midlatitude stormtracks [5].

REFERENCES

- [1] Bjerknes, J., *Saturated-adiabatic ascent of air through dry- adiabatically descending environment*. Quart. J. Roy. Meteor. Soc. **64** (1938), 325–330.
- [2] D.G. Andrews, J.R. Holton, and C.B. Leovy, *Middle Atmospheric Dynamics*. International Geophysics Series, **40** (1987), 489 pp
- [3] Pauluis, O., A. Czaja and R. Korty, *The global atmospheric circulation on moist isentropes*, Science **321** (2008), 1075–1078.
- [4] Pauluis, O., A. Czaja and R. Korty, *The global atmospheric circulation in moist isentropic coordinates*, J. Climate **23** (2010), 3077–3093.
- [5] R. Yamada and O. Pauluis, *Momentum balance and Eliassen-Palm flux on moist isentropic surfaces*, J. Atmos. Sci. **72** (2015), 2070–2089.

Self-Aggregation of atmospheric convection in idealized simulations

CAROLINE MULLER

(joint work with Sandrine Bony)

This project aims at improving our understanding of atmospheric deep convection and its spatial organization. Organized convection, for instance, squall lines or tropical cyclones, with their associated clouds, strong precipitation and winds, can cause severe material damage and can be deadly. The organization of clouds is ubiquitous in the tropics, but is not well understood. One particular type of convective organization in cloud-resolving simulations in idealized settings that has

received attention recently is the self-aggregation of convection [1, 8, 2, 3] (Fig. 1), taking the form of cloud clusters, or tropical cyclones in the presence of rotation.

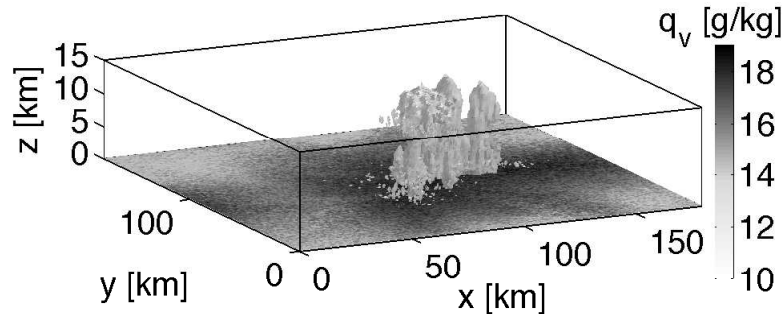


FIGURE 1. Clouds (white surfaces) and near-surface water vapor mixing ratio (first atmospheric level at 37.5 m in colors) at the end of a simulation in which the convection self-aggregates into a single convective region. Adapted from [7]

The processes leading to self-aggregation in idealized simulations may play an important role in cyclogenesis [5], but the conditions that favor self-aggregation are still unclear. We use high-resolution cloud-resolving simulations to investigate in detail the physical process responsible for the aggregation, and how aggregation couples to a large-scale circulation. We find that various feedbacks can lead to aggregation: interactive longwave cooling from low-level clouds; interactive longwave cooling from high clouds and clear sky; and a moisture-memory feedback in humid conditions, i.e. when the evaporative-driven downdrafts below deep clouds are weak. Aggregation is accompanied by large changes in the large-scale thermodynamic and radiative properties [7].

It has been recently suggested that the self-aggregated state could be the preferred stable equilibrium of tropical convection under warm sea-surface temperatures [4, 6]. With changing climate, the tropics could switch to this self-aggregated state. Given the large changes in large-scale properties accompanying self-aggregation, this has important implications for climate sensitivity.

REFERENCES

- [1] Bretherton, C. S., P. N. Blossey, and M. Khairoutdinov (2005), *An energy-balance analysis of deep convective self-aggregation above uniform SST*, J. Atmos. Sci., **62**, 4273–4292.
- [2] Craig, G. C., and J. M. Mack (2013), *A coarsening model for self-organization of tropical convection*, J. Geophys. Res., **118**, 8761–8769.
- [3] Emanuel, K. A., A. A. Wing, and E. M. Vincent (2014), *Radiative-convective instability*, J. Adv. Model. Earth Syst., *6*(1), 75–90.
- [4] Khairoutdinov, M. F., and K. A. Emanuel (2010), *Aggregated convection and the regulation of tropical climate*, Preprints, 29th conference on Hurricanes and Tropical Meteorology, Tucson, AZ, Amer. Meteor. Soc., **P2.69**.
- [5] Khairoutdinov, M., and K. Emanuel (2013), *Rotating radiative-convective equilibrium simulated by a cloud-resolving model*, J. Adv. Model. Earth Syst., **5**, 816–825.
- [6] Mauritsen, T., and B. Stevens (2015), *Missing iris-effect as a possible cause of high climate sensitivity in models*, Nature Geosci., **8**, 346–351.

- [7] Muller, C., S. Bony (2015), *What favors convective aggregation, and why?*, *Geophys. Res. Lett.* **42**, 5626–5634.
- [8] Muller, C. J., and I. M. Held (2012), *Detailed investigation of the self-aggregation of convection in cloud-resolving simulations*, *J. Atmos. Sci.*, **69**, 2551–2565.
- [9] M. Muster, *Computing certain invariants of topological spaces of dimension three*, *Topology* **32** (1990), 100–120.

Mesoscale and Sub-Mesoscale Wave Dynamics Throughout all Atmospheric Layers

ULRICH ACHATZ

Various aspects of research on the dynamics of small-scale waves in the atmosphere have been reported:

(1) The interaction between locally monochromatic finite-amplitude mesoscale waves, their nonlinearly induced higher harmonics, and a synoptic-scale flow has been reconsidered, both in the tropospheric regime of weak stratification and in the stratospheric regime of moderately strong stratification. A review of the basic assumptions of quasi-geostrophic theory on an f -plane yields all synoptic scales in terms of a minimal number of natural variables, i.e. two out of the speed of sound, gravitational acceleration and Coriolis parameter. The wave scaling has been defined so that all spatial and temporal scales are shorter by one order in the Rossby number, and by assuming their buoyancy field to be close to static instability. WKB theory is applied, with the Rossby number as scale separation parameter, combined with a systematic Rossby-number expansion of all fields. Classic results for synoptic-scale-flow balances and inertia-gravity wave (IGW) dynamics have been recovered. These are supplemented by explicit expressions for the interaction between mesoscale geostrophic modes (GM), a possibly somewhat overlooked agent of horizontal coupling in the atmosphere, and the synoptic-scale flow. It has been shown that IGW higher harmonics are slaved to the basic IGW, and that their amplitude is one order of magnitude smaller than the basic-wave amplitude. GM higher harmonics are not that weak and they are in intense nonlinear interaction between themselves and the basic GM. Compressible dynamics plays a significant role in the stratospheric stratification regime, where anelastic theory would yield insufficient results. Supplementing classic derivations, it is moreover shown that in the absence of mesoscale waves quasi-geostrophic theory holds also in the stratospheric stratification regime. For details see [1].

(2) The comparative relevance in gravity-wave (GW) drag of direct GW-mean-flow interactions and turbulent wave breakdown have been investigated [2]. Of equal interest have been how well Wentzel-Kramer-Brillouin (WKB) theory can capture direct wave-mean-flow interactions, that are excluded by applying the steady-state approximation. WKB has been implemented in a very efficient Lagrangian ray-tracing approach that considers wave-action density in phase-space, thereby avoiding numerical instabilities due to caustics. It has been supplemented by a simple wave-breaking scheme based on a static-instability saturation criterion. Idealized test cases of horizontally homogeneous GW packets have been

considered where wave-resolving Large-Eddy Simulations (LES) provide the reference. In all of these cases the WKB simulations including direct GW-mean-flow interactions reproduce the LES data, to a good accuracy, already without wave-breaking scheme. The latter provides a next-order correction that is useful for fully capturing the total-energy balance between wave and mean flow. Moreover, a steady-state WKB implementation, as used in present GW parameterizations, and where turbulence provides, by the non-interaction paradigm, the only possibility to affect the mean flow, is much less able to yield reliable results. The GW energy is damped too strongly and induces an oversimplified mean flow. This argues for WKB approaches to GW parameterization that take wave transience into account.

(3) An on-line GW parameterization has been implemented in a linear but global model that incorporates their horizontal propagation, the effects of transients and of horizontal background gradients on GW dynamics [3]. The GW parameterization is based on a ray-tracer model with a spectral formulation that is safe against numerical instabilities due to caustics. The global model integrates the linearized primitive equations to obtain solar tides (STs), with a seasonally dependent reference climatology, forced by a climatological daily cycle of the tropospheric and stratospheric heating, and the (instantaneous) GW momentum and buoyancy flux convergences resulting from the ray-tracer. Under a more conventional “*single-column*” approximation, where GWs only propagate vertically and do not respond to horizontal gradients of the resolved flow, GW impacts are shown to be significantly changed in comparison with “full” experiments, leading to significant differences in ST amplitudes and phases, pointing at a sensitive issue of GW parameterizations in general. In the “full” experiment, significant semi-diurnal STs arise even if the tidal model is only forced by diurnal heating rates. This indicates that an important part of the tidal signal is forced directly by GWs via their momentum and buoyancy deposition. In general the effect of horizontal GW propagation and the GW response to horizontal large-scale-flow gradients is rather observed in non-migrating than in migrating tidal components. This shows that lateral-propagation effects of GWs, presently neglected in GW parameterizations, are important in the mesosphere and higher.

(4) Work is in progress on the efficient description of sub-mesoscale GWs in models resolving mesoscale flow. A WKB theory has been developed that describes this situation. Numerical simulations seem to well reproduce the generation of a mesoscale GWs by a submesoscale GW packet. This might eventually be relevant for subgrid-scale parameterizations in numerical weather prediction.

REFERENCES

- [1] U. Achatz and B. Ribstein and F. Senf and R. Klein, *The interaction between synoptic-scale balanced flow and a finite-amplitude mesoscale wave field throughout all atmospheric layers: Weak and moderately strong stratification*, Q. J. R. Met. Soc. **submitted** (2016).
- [2] G. Boloni, B. Ribstein, J. Muraschko, C. Sgoff, J. Wei, and U. Achatz, *The interaction between atmospheric gravity waves and large-scale flows: an efficient description beyond the non-acceleration paradigm*, J. Atmos. Sci. **accepted**.

- [3] B. Ribstein and U. Achatz, *he interaction between gravity waves and solar tides in a linear tidal model with a 4D ray-tracing gravity-wave parameterization*, *J. Geophys. Res. Space Physics* **121** (2016) 1–15.

Scattering of the Internal Tide by Balanced Flow

WILLIAM R. YOUNG

(joint work with Gregory L. Wagner and Gwenaël Ferrando)

Starting from the hydrostatic Boussinesq equations we derive a phase-averaged asymptotic equation describing the propagation of inertia-gravity waves through three-dimensional quasi-geostrophic flow with non-uniform background density stratification. The derivation uses a multiple-scale asymptotic method based on the assumption that the wave field has a single well-defined frequency σ . In the oceanographic problem motivating this development, σ is the frequency of the semi-diurnal lunar tide. The asymptotic development neglects nonlinear wave-wave interactions, and makes no restriction on the relative spatial scale between waves and quasi-geostrophic flow.

The leading order pressure is represented as

$$(1) \quad p_0 = f_0 (\psi + Ae^{-i\sigma t} + A^*e^{i\sigma t}) ,$$

where f_0 is the local Coriolis frequency and $\psi(x, y, z, t)$ is the quasigeostrophic stream function of the balanced flow. The complex field $A(x, y, z, t)$ encodes the slow evolution of the internal tide. An unconventional asymptotic expansion results in the phase-averaged evolution equation

$$(2) \quad \begin{aligned} EA_t + J(\psi, EA) + J(\psi_x, A_x) + J(\psi_y, A_y) - \frac{f_0^2}{2\sigma^2} J(D\psi, A) \\ + i\frac{f_0}{2\sigma} \{ \nabla \cdot (D\psi \nabla A) + 2J(\psi_x, A_y) - 2J(\psi_y, A_x) \} \\ + i\frac{f_0^2}{2\sigma} \frac{\sigma^2 - f_0^2}{f_0^2} \{ DA + \partial_z (\zeta DA) - D(\zeta A_z) \} = 0. \end{aligned}$$

In (2), ∇ is the horizontal gradient, $\zeta = f_0\psi_z/N^2$ is the vertical displacement of buoyancy surfaces by the balanced flow and D and E are second-order differential operators defined as

$$(3) \quad D = \partial_x^2 + \partial_y^2 - \frac{\sigma^2 - f_0^2}{f_0^2} \partial_z \frac{f_0^2}{N^2} \partial_z ,$$

and

$$(4) \quad E = \frac{\sigma^2 - f_0^2}{4\sigma^2} \left[\partial_x^2 + \partial_y^2 + \frac{3\sigma^2 + f_0^2}{f_0^2} \partial_z \frac{f_0^2}{N^2} \partial_z \right] .$$

Comparison of numerical solutions of the hydrostatic Boussinesq equations with solutions of (2) show that (2) is accurate provided that the wave frequency σ is not close to the Coriolis frequency f_0 and that the quasi-geostrophic flow is not too vigorous — see figure 1. Specifically the approximation requires that

$$(5) \quad \frac{U}{f_0 L} \frac{\sigma^2}{\sigma^2 - f_0^2} \ll 1 .$$

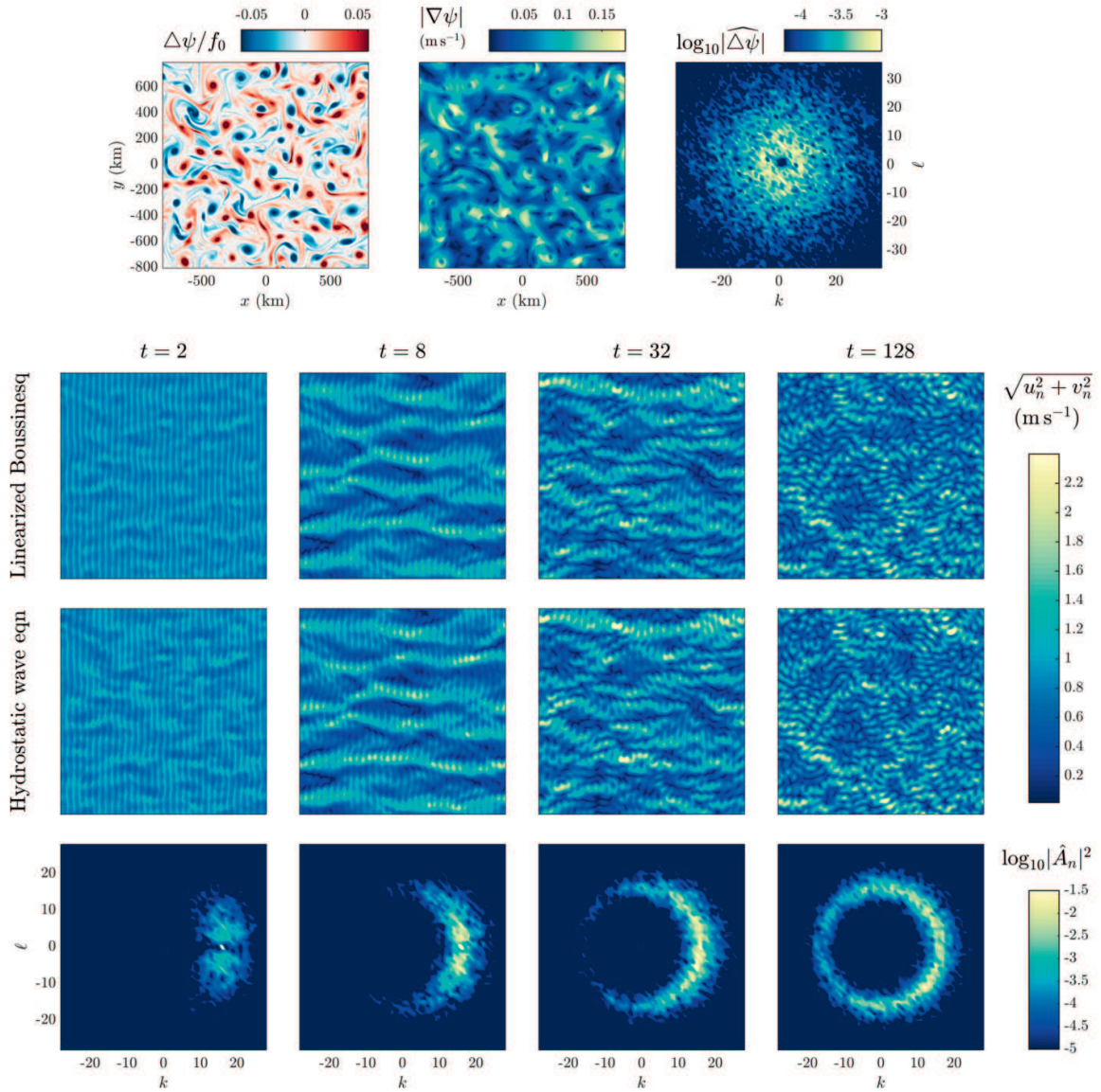


FIGURE 1. Scattering of a plane wave by two-dimensional turbulence with maximum vorticity $0.14f_0$ and root-mean-square vorticity $0.024f_0$. The top 3 panels show the initial turbulent vorticity, speed, and the periodogram of vorticity. The bottom 12 panels show the evolution of an initially horizontal plane wave scattered by the turbulent fields at top: the first row shows speed in the linearized hydrostatic Boussinesq system; the second row shows speed in the hydrostatic wave equation (2); and the third row shows the Fourier components of A in (2). Time is in inertial periods.

Above U/f_0L is the Rossby number of the balanced flow. The comparison in figure 1 shows close agreement between solutions of the Boussinesq equations and (2).

Multiscale Methods in Strongly Anisotropic Geophysical Systems

KEITH JULIEN

Fluid flows in planetary and stellar interiors can be broadly characterized as rapidly rotating, and turbulent (and when appropriate constrained by strong magnetic forces). In non-dimensional parameter space such flows reside in the low Rossby number, large Reynolds number limit. Direct numerical simulations (DNS) of the complete set of governing equations are now routine practice for fluid turbulence, but remain limited to parameter values that are quite distant from natural systems owing to the massive requirements for numerically resolving disparate spatiotemporal scales. Improvements in computing power through Moore's laws will produce minimal advances with present-day models. Moreover, the paucity of observational data limit the development and verification of strategies that parameterizes small-scale turbulent motions in hope of providing some computational relief. It is therefore clear that advances must occur through new model development and associated simulations utilizing extreme parameter values in an asymptotic manner. The stiff character of the governing equations, while an impediment to DNS, provides a possible path forward for simplifying, or reducing, the governing equations with the use of multiscale asymptotics [1, 2]. Balanced flows, in which two or more forces in the momentum equations are in balance, are particularly suitable for asymptotic analysis given the subdominance of inertial accelerations. Indeed, reduced models based on the geostrophic balance, in which the Coriolis and pressure gradient forces balance, have formed the backbone for theoretical and numerical investigations on the large-scale stably-stratified dynamics of the Earth's atmosphere and oceans for over 60 years [3, 4]. Recently, advances have illustrated how such an approach can be extended to convectively unstable environments appropriate for planetary and stellar interiors. The methodology parallels classical quasigeostrophic theory but is generalized to flows with spatial anisotropies that are columnar rather than pancake-like.

The result of asymptotic modeling approach is the non-hydrostatic quasi-geostrophic (NH-QG) equations [5]. The system bears all the hall-marks of classical QG: point-wise geostrophic balance; nonlinear flow advection that is dominant in planes perpendicular to the rotation axis and a linear vortex-stretching force that drives vortical motions. However, central differences also exists. Strong vertical motions occur that are comparable in magnitude to horizontal motions, as a result vertical motions are no longer diagnostic but must be evolved prognostically. It is also found that unlike classical QG (which filters all inertial wave-motions) the model retains slow inertial (columnar) waves as a consequence of the weakly stratified environment. These waves propagate predominantly in horizontal directions whilst wave-energy propagated by the group velocity is transmitted predominantly in the vertical direction. Columnar anisotropy also captures dissipative effect in the horizontal directions that enables the tracking of fluid motions from laminar through to the turbulent regime. Dissipation in the vertical direction remains subdominant and without any further corrections the model automatically enforces any horizontal boundary to be impenetrable stress-free.

The goal of the present investigation is quantitatively evaluate the reduced NH-QG model in the setting of rotating Rayleigh-B'énard convection in plane layer [6, 7]. The fidelity of the model, obtained by an asymptotic reduction of the Navier-Stokes equations, is explored for the first time by comparisons of simulations against the findings of direct numerical simulations (DNS) and laboratory experiments of rotationally constrained convection. Comparisons focus on flow morphology and transitions and global heat transport as a function of thermal forcing. Excellent agreement is found for the case of stress-free boundary conditions for maximal values of the rotation rate attainable in experiments and DNS, as measured by Ekman number $E \approx 10^{-7}$. In the more realistic laboratory setting of no-slip boundaries large discrepancies between the NH-QG model and companion laboratory and DNS studies. Ekman pumping is found to be the source of this discrepancy. Results from numerical simulations of three-dimensional rotating Rayleigh-Bénard convection are discussed using an updated asymptotic quasi-geostrophic model that incorporates the effects of no-slip boundaries through (i) parameterized Ekman pumping boundary conditions, and (ii) a thermal wind boundary layer that regularizes the enhanced thermal fluctuations induced by pumping. For $E \approx 10^{-7}$, excellent agreement is achieved for fluids with Prandtl number $Pr = 1$ and good qualitative agreement is achieved for $Pr > 1$. Similar to studies with stress-free boundaries, four spatially distinct flow morphologies exists, each in geostrophic balance. Despite the presence of frictional drag at the upper and lower boundaries, a strong non-local inverse cascade of barotropic (i.e., depth-independent) kinetic energy persists in the final regime of geostrophic turbulence and is dominant at large scales. For mixed no-slip/stress-free and no-slip/no-slip boundaries, Ekman friction is found to attenuate the efficiency of the upscale energy transport and, unlike the case of stress-free boundaries, rapidly saturates the barotropic kinetic energy. For no-slip/no-slip boundaries, Ekman friction is strong enough to prevent the development of a coherent dipole vortex condensate. Instead vortex pairs are found to form intermittently before being destroyed frictionally. For all combinations of boundary conditions, a Nastrom-Gage type spectrum of kinetic energy is found where the power law exponent changes from ≈ -3 to $\approx -5/3$, i.e. from steep to shallow, as the spectral wavenumber increases.

REFERENCES

- [1] Julien, K. and Knobloch, E., *Reduced models for fluid flows with strong constraints*, J. Math. Phys. **48** (2007) 065405.
- [2] Klein, R., *Scale-dependent models for atmospheric flows*, Ann. Rev. Fluids. **42**, (2010) 249-274.
- [3] Charney, J.G., *Geostrophic turbulence*, J. Atmos. Sci. **28**, (1971) 1087-1095.
- [4] Pedlosky, J., *Geophysical Fluid Dynamics*, (1987).
- [5] Julien, K., Knobloch, E., Milliff, R. and Werne, J., *Generalized quasi-geostrophy for spatially anisotropic rotationally constrained flows*, J. Fluid Mech. **555**, (2006) 233-274.
- [6] Julien, K., Aurnou, J., Calkins, M.A, Marti, P., Stellmach, S. and Vasil, G.M., *A nonlinear model for rotationally constrained convection with Ekman pumping.*, J. Fluid Mech. **798**, (2016) 50-87.

- [7] Plumley, M., Julien, K., Marti, P. and Stellmach, S., *The Effect of Ekman pumping on Quasigeostrophic Rayleigh-Benard Convection.*, J. Fluid Mech. **803**, (2016) 51-71.

Multiscale asymptotics for the Madden-Julian oscillation and tropical-extratropical interactions

SAMUEL N. STECHMANN

The results of two papers are presented.

First [1], a new model is derived and analyzed for tropical-extratropical interactions involving the Madden-Julian oscillation (MJO). The model combines (i) the tropical dynamics of the MJO and equatorial baroclinic waves and (ii) the dynamics of barotropic Rossby waves with significant extratropical structure, and the combined system has a conserved energy. The method of multiscale asymptotics is applied to systematically derive a system of ordinary differential equations (ODEs) for three-wave resonant interactions. Two novel features are (i) a degenerate auxiliary problem with overdetermined equations due to a compatibility condition (meridional geostrophic balance) and (ii) cubic self-interaction terms that are not typically found in three-wave resonance ODEs. Several examples illustrate applications to MJO initiation and termination, including cases of (i) the MJO, equatorial baroclinic Rossby waves, and barotropic Rossby waves interacting, and (ii) the MJO, baroclinic Kelvin waves, and barotropic Rossby waves interacting. Resonance with the Kelvin wave is not possible here if only dry variables are considered, but it occurs in the moist model here through interactions with water vapor and convective activity.

Second [2], two kinds of additional interactions are illustrated in the model: (i) MJO initiation through extraction of energy from barotropic Rossby waves and (ii) MJO termination via energy transfer to extratropical Rossby waves. A new feature, in comparison to previous simplified models, is that here these waves interact directly in the presence of a climatological mean flow given by the Walker circulation. The simplified models are systems of ordinary differential equations (ODEs) for the amplitudes of barotropic Rossby waves and the MJO, and they are systematically derived from the MJO skeleton model by using multiscale asymptotics. The simplified ODEs allow for rapid investigation of a wide range of model parameters, such as initial conditions and wind shear. Zonally uniform wind shear is shown to have only a minor effect on these interactions here, in contrast to the important role of the zonally varying wind shear associated with the Walker circulation. The models illustrate some realistic features of tropical-extratropical interactions on intraseasonal to seasonal time scales. A key aspect of the models here is that the water vapor and convective activities are interactive components of the model, rather than specified external heating sources.

REFERENCES

- [1] S. Chen, A. J. Majda, S. N. Stechmann, *Multiscale asymptotics for the skeleton of the Madden-Julian oscillation and tropical-extratropical interactions*, *Math. Clim. Weather Forecast.* **1** (2015), 43–69.
- [2] S. Chen, A. J. Majda, S. N. Stechmann, *Tropical-extratropical interactions with the MJO skeleton and climatological mean flow*, *J. Atmos. Sci.* **in press**.

Beyond the limit of infinite time-scale separation: Edgeworth approximations and homogenisation

GEORG A. GOTTWALD

(joint work with Jeroen Wouters)

Homogenization has been widely used in stochastic model reduction of slow-fast systems, including geophysical and climate systems [4]. From a modelling perspective, current challenges in homogenization include how to deal with the situation when the slow variables couple back into the fast dynamics. Furthermore, the theory relies on an infinite time scale separation [5, 2, 3]. In this talk we present results for the realistic case of finite time scale separation. In particular, we employ Edgeworth expansions [1] as finite size corrections to the central limit theorem and show improved performance of the reduced stochastic models in numerical simulations.

The Edgeworth expansion is a finite size correction of the central limit theorem. We show how the Edgeworth expansion improves the estimation of the empirical density of finite Birkhoff sums of variables generated by an AR1 process as well as for hyperbolic chaotic deterministic maps.

We then introduce a stochastic surrogate process the parameters of which are tuned to match the higher-order finite size corrections required by the Edgeworth expansion. We compare reduced model statistics of our Edgeworth reduced system with those employing solely the central limit theorem (or homogenisation). The improvement is remarkable, in particular for the skewness.

Finally, we study a multi-scale triad system. The system is of the form of geophysical fluid dynamic equations with quadratic energy conserving nonlinearities such as in the barotropic vorticity equation. We replace the fast stochastic part of the equations with a surrogate process where the parameters are chosen to match the Edgeworth statistics of the triad system which can be analytically computed. The improvement of the first moments is notable when compared to classical homogenisation. The results have been shown to be closely related to the recent approach by Wouters et al [6] which uses response theory to match the statistics rather than the Edgeworth expansion. Therein, however, a free parameter appeared which is fixed by the Edgeworth expansion.

This is joint work with Jeroen Wouters.

REFERENCES

- [1] F.Götze and C. Hipp, *Asymptotic expansions for sums of weakly dependent random vectors*, Z. Wahrscheinlichkeitstheorie verw. Gebiete **64** (1983) 211-239.
- [2] G.A. Gottwald and I. Melbourne, *Homogenization for deterministic maps and multiplicative noise*, Proceedings of the Royal Society A: Mathematical, Physical and Engineering Science **469** (2013).
- [3] D. Kelly and I. Melbourne, *Deterministic homogenization for fast-slow systems with chaotic noises*, (2014) submitted.
- [4] A.J. Majda, I. Timofeyev and E. Vanden Eijnden, *A priori tests of a stochastic mode reduction strategy*, Proceedings of the National Academy of Sciences **26**, (1999), 14687-14691.
- [5] I. Melbourne and A. Stuart, *A note on diffusion limits of chaotic skew-product flows*, Nonlinearity **24** (2011) 1361–1367.
- [6] J. Wouters et al, *Parametrization of stochastic multiscale triads*, Nonlin. Processes Geophys. Discuss., doi:10.5194/npg-2016-37, in review, 2016.

A Gaussian-product stochastic Gent-McWilliams parameterization

IAN GROOMS

Computational ocean models play a crucial role in modern oceanography, simultaneously encoding and extending our understanding, and supporting policy decisions on everything from fisheries to long-term climate change. Global ocean models (hereinafter OGCMs, ocean general circulation models) are an important class of ocean models, and one of the foremost obstacles to developing accurate GCMs is the inability to completely resolve mesoscale eddy dynamics (10–100 km horizontal scales). Mesoscale eddies are the most energetic ocean feature, and play a large role in air-sea interaction and in low frequency variability of the ocean. Representation of the effects of these unresolved eddies in global ocean models is crucial for obtaining accurate simulations.

The primary impact of unresolved dynamics in non-eddy-resolving GCMs is the transport of tracers and momentum. In regions where mesoscale eddy dynamics are completely unrepresented, the primary subgrid-scale transport is of tracers, and in regions where the eddy dynamics are partially represented but incompletely resolved the primary subgrid-scale transport is of momentum. In regions where eddies are completely unresolved (which in some models includes the entire global ocean), the dominant parameterization paradigm is the Gent-McWilliams framework (GM: [6, 7]) which essentially codifies the well-established properties of mesoscale eddies to transport tracers along isopycnals and to reduce potential energy by flattening isopycnals. (Mesoscale eddies also mix tracers along isopycnal directions; this effect is parameterized separately from GM.) The GM parameterization drains potential energy; though it leads to reasonable mean states, GM-parameterized models lack realistic variability. Ensemble methods for state estimation, forecasting, and uncertainty quantification use non-eddy-resolving models because of computational expense, and lack sufficient variability to perform correctly.

Mesoscale eddy dynamics are turbulent, and the eddies produce chaotic time series of tracer fluxes even when averaged over the scale of the computational grid of a coarse OGCM. The fact that the real fluxes are chaotic implies that a realistic parameterization should be stochastic. Very little work has been done to develop stochastic parameterizations for coarse, non-eddy-permitting models. Brankart[2] developed a stochastic parameterization associated with the joint effect of eddy variability and the nonlinear equation of state of seawater, and Grooms et al.[4] applied a multiscale stochastic approach to a non-eddy-permitting quasi-geostrophic (QG) model. The only other approach (known to the author) is the generic approach of Buizza et al.[5], where the coefficients in existing deterministic parameterizations are multiplied by random fields; this approach has come to be known as “stochastically perturbed physics tendencies” (here SPPT), and has been applied in non-eddy-permitting ocean models with mixed results by Andrejczuk et al.[1] and Brankart et al.[3].

The goal of the present investigation is to develop a stochastic parameterization for tracer transport in non-eddy-permitting cases that is based around the widespread and (relatively) successful GM framework. Distilled to its essence, the parameterization involves the development of Gaussian random field models for subgrid-scale variables (eddy velocity and density anomalies), then the construction of a stochastic subgrid-scale density flux by multiplying these Gaussian random fields. Our parameterization is also temporally smooth so that, though stochastic, it is still compatible with the smoothness assumptions associated with the time-discretizations used in numerical ocean models. This stochastic flux is then placed in the GM framework to produce a stochastic quasi-Stokes eddy-induced velocity field.

A preliminary version of the stochastic GM parameterization is developed where the structure of the random fields is significantly simplified: the vertical structure is parameterized; the spatial correlations are stationary and isotropic; and the spatio-temporal covariance is separable. The formulation has the advantage that the mean flux, conditioned on the resolved variables, can be made equal to any of the many existing formulations of the GM parameterization. Several stochastic parameterizations based on the approach of Buizza et al.[5] are also developed for comparison.

The stochastic parameterizations are tested in a double-gyre scenario, forced by wind stress and a temperature-restoring boundary condition at the surface (an inhomogeneous Neumann condition on velocity, and inhomogeneous Robin condition on temperature). The Gaussian-product parameterization has marked qualitative differences in comparison with the deterministic and Buizza et al.[5] parameterizations. The overturning circulation is much stronger, the net kinetic energy is much higher, the local temperature variability is greater, etc.

An eddy-resolving simulation was not available for comparison, so it is not clear whether the increased variability is realistic. As an a priori test of the stochastic parameterization, coarse-grained flux statistics were computed from doubly-periodic QG simulations of mesoscale eddies. The observed statistics are very

close to the Gaussian-product distribution, except in cases where the eddy scales are smaller than the averaging scale (even in those cases the flux distributions were very non-Gaussian). Thus, the Gaussian-product stochastic parameterization are at least known to be more consistent with observed fluxes than the Buizza et al.[5] parameterizations.

In the future we plan to make the Gaussian random field models more realistic, though this will require careful selection or development of strategies for sampling non-stationary, inhomogeneous Gaussian random fields. We also plan to incorporate the effects of averaging into the parameterization, since the observed flux distribution is not product-normal when the eddy scales are smaller than the coarse grid scale. An eddy-resolving simulation is being spun up for comparison, and we hope to test whether the new parameterization leads to improvements in ensemble data assimilation.

REFERENCES

- [1] Andrejczuk, M., Cooper, F., Juricke, S., Palmer, T., Weisheimer, A., Zanna, L., 2015. Oceanic stochastic parametrizations in a seasonal forecast system. arXiv preprint arXiv:1506.09181 .
- [2] Brankart, J.M., 2013. Impact of uncertainties in the horizontal density gradient upon low resolution global ocean modelling. *Ocean Model.* **66**, 64–76.
- [3] Brankart, J.M., Candille, G., Garnier, F., Calone, C., Melet, A., Bouttier, P.A., Brasseur, P., Verron, J., 2015. A generic approach to explicit simulation of uncertainty in the nemo ocean model. *Geoscientific Model Development* **8**, 1285–1297.
- [4] Grooms, I., Majda, A.J., Smith, K.S., 2015b. Stochastic superparameterization in a quasi-geostrophic model of the Antarctic Circumpolar Current. *Ocean Model.* **85**, 1–15.
- [5] Buizza, R., Milleer, M., Palmer, T., 1999. Stochastic representation of model uncertainties in the ecmwf ensemble prediction system. *Quarterly Journal of the Royal Meteorological Society* **125**, 2887–2908.
- [6] Gent, P.R., McWilliams, J.C., 1990. Isopycnal mixing in ocean circulation models. *J. Phys. Ocean.* **20**, 150–155.
- [7] Gent, P.R., Willebrand, J., McDougall, T.J., McWilliams, J.C., 1995. Parameterizing eddy-induced tracer transports in ocean circulation models. *J. Phys. Ocean.* **25**, 463–474.

Applications of optimization and optimal control to some fundamental problems in mathematical fluid dynamics

CHARLES DOERING

Optimization and optimal dynamical control are used to investigate the accuracy of analytical estimates for solutions of some basic nonlinear partial differential equations of mathematical hydrodynamics. Even though many mathematical estimates are demonstrably sharp, the result of a sequence of applications of such estimates need not be sharp leaving uncertainty in the ultimate result of the analysis. We examine the classical analysis bounding enstrophy [1, 2] and palinstrophy [3] amplification in Burgers' and the Navier-Stokes equations and discover that the best known instantaneous growth rates estimates are indeed sharp. But integrating the estimates in time does not always produce sharp estimates in which case optimal control techniques must be brought to bear to determine the actual

extreme behavior of the nonlinear dynamics. The question of 3D Navier-Stokes regularity remains unanswered although work is in progress to apply these tools to the challenge [4].

REFERENCES

- [1] L. Lu and C. R. Doering, *Limits on enstrophy growth for solutions of the three-dimensional Navier-Stokes equations*, Indiana University Mathematics Journal **57** (2008), 2693–2727.
- [2] D. Ayala and B. Protas, *On maximum enstrophy growth in a hydrodynamic system*, Physica D **240** (2011), 1553–1563.
- [3] D. Ayala and B. Protas, *Vortices, maximum growth and the problem of finite-time singularity formation*, Fluid Dynamics Research **46** (2014), 031404.
- [4] C. R. Doering, *The 3D Navier-Stokes Problem*, Annual Review of Fluid Mechanics **41** (2009), 109–128.

Compressible Navier-Stokes Equations with Density Dependent Viscosities

DIDIER BRESCH

P. Gent published in 1993 an article in *J. Atmos. Sci.* where he discussed energetically consistent viscous shallow-water equations proposing the following version

$$\begin{aligned}\partial_t h + \operatorname{div}(hu) &= 0, \\ \partial_t(hu) + \operatorname{div}(hu \otimes u) - 2\nu \operatorname{div}(hD(u)) + h\nabla h &= 0\end{aligned}$$

with $D(u) = (\nabla u + \nabla^t u)/2$ and where h denotes the height and u the horizontal mean velocity. Note that a similar system has been mathematically justified from incompressible Navier-Stokes equations with free surface in [6].

A two-velocities Hydrodynamic. It is interesting to note that such version, proposed by P. Gent, is energetically consistent namely provides the relation

$$\frac{1}{2} \frac{d}{dt} \int_{\Omega} (h|u|^2 + h^2) + 2 \int_{\Omega} h|D(u)|^2 = 0$$

but also presents a two-velocities hydrodynamic formulation. To see that, it suffices to take the gradient of the mass equation: it reads

$$\partial_t(\nabla h) + \operatorname{div}(\nabla h \otimes u) + \operatorname{div}(h\nabla^t u) = 0$$

which may be written under the form

$$\partial_t(h\nabla \log h) + \operatorname{div}(h\nabla \log h \otimes u) + \operatorname{div}(h\nabla^t u) = 0.$$

Thus $U = u + 2\nu\nabla \log h$ satisfies the equation

$$\partial_t(hU) + \operatorname{div}(hU \otimes u) - 2\nu \operatorname{div}(hA(U)) + h\nabla h = 0$$

where

$$A(U) = (\nabla U - \nabla^t U)/2.$$

Taking the scalar product of this equation with U and integrating in space, we get

$$\frac{1}{2} \frac{d}{dt} \int_{\Omega} (h|U|^2 + h^2) + 2 \int_{\Omega} h|A(U)|^2 + \nu \int_{\Omega} |2\nabla h|^2 = 0.$$

It may be seen as a nonlinear hypocoercivity property for the compressible Navier-Stokes equations due to the density dependency of the viscosity. This case has attracted a lot of attention since the discovering by D.B. and B. Desjardins of this new entropy (called now BD entropy) which provides new a priori estimates on the gradient of the density. The reader is referred to [4] for a chapter on the subject. Recently, Bresch Desjardins and Zatorska showed that the system can be reformulated through an augmented system (via the so-called kappa entropy). It explains how the additional control on the density is linked to a hidden bi-fluid structure of the system.

Using a parameter $\kappa \in (0, 1)$, we can mix the energy estimates and the estimate given above to write a kind of two-velocities hydrodynamic estimate (a κ -entropy as called in [5]):

$$\begin{aligned} & \frac{1}{2} \frac{d}{dt} \int_{\Omega} ((1 - \kappa)h|u|^2 + \kappa h|U|^2 + h^2) \\ & + 2 \int_{\Omega} (1 - \kappa)h|D(u)|^2 + 2 \int_{\Omega} \kappa h|A(U)|^2 + \kappa \nu \int_{\Omega} |2\nabla h|^2 = 0. \end{aligned}$$

Note that

$$(1 - \kappa)h|u|^2 + \kappa h|U|^2 = h(|u + 2\kappa\nu\nabla \log h|^2 + \kappa(1 - \kappa)|2\nu\nabla \log h|^2)$$

and therefore we can write the system satisfied by

$$(h, V, W) = (h, u + 2\kappa\nu\nabla \log h, 2\sqrt{\kappa(1 - \kappa)}\nu\nabla \log h)$$

which reads

$$\begin{aligned} \partial_t h + \operatorname{div}(hu) &= 0, \\ \partial_t(hV) + \operatorname{div}(hV \otimes u) + h\nabla h &= \nu \operatorname{div}(2h(1 - \kappa)D(V)) \\ &\quad + \nu \operatorname{div}(2\kappa A(V)) - \nu \operatorname{div}(2\sqrt{\kappa(1 - \kappa)}h\nabla W) \\ \partial_t(hW) + \operatorname{div}(hW \otimes u) &= \nu \operatorname{div}(2\kappa h\nabla W) \\ &\quad - \nu \operatorname{div}(2\sqrt{\kappa(1 - \kappa)}h\nabla^t V) \end{aligned}$$

It is interesting to note that the bi-fluid structure observed by D. B. with B. Desjardins and E. Zatorska is included in a mono-fluid system. This has to be compared to the discussions by H. Brenner in [1], [2]: See [10] for the mathematical study of Brenner's systems.

Note that similar formulations may be obtained for a more general PDEs than the viscous shallow-water system namely it may be obtained for the compressible Navier-Stokes system

$$\begin{aligned} \partial_t \rho + \operatorname{div}(\rho u) &= 0, \\ \partial_t(\rho u) + \operatorname{div}(\rho u \otimes u) - 2\nu \operatorname{div}(\mu(\rho)D(u)) - \nabla(\lambda(\rho)\operatorname{div}u) + \nabla p(\rho) &= 0 \end{aligned}$$

if μ and λ are related to the following algebraic relation

$$\lambda(\rho) = 2(\mu'(\rho)\rho - \mu(\rho)).$$

The interested reader is referred to [3] for more details. Actually no physical explanation exists regarding the relation between λ and μ but it is really interesting to see that such constraint may also appear in the Euler-Korteweg system.

Euler-Korteweg: A two-velocities hydrodynamic? This has been observed recently in [8]. Let us start with the energy for Euler-Korteweg namely

$$\int_{\Omega} \frac{1}{2} \rho |u|^2 + \rho e(\rho) + \kappa(\rho) |\nabla \rho|^2$$

with a density ρ satisfying the mass equation

$$\partial_t \rho + \operatorname{div}(\rho u) = 0.$$

Then the associated Euler-Lagrange equation reads

$$\partial_t(\rho u) + \operatorname{div}(\rho u \otimes u) + \nabla p(\rho) = \operatorname{div} K$$

with

$$K = \left(\rho \operatorname{div}(K(\rho \nabla \rho)) + \frac{1}{2} (K(\rho) - \rho K'(\rho) |\nabla \rho|^2) \right) \operatorname{Id} - K(\rho) \nabla \rho \otimes \nabla \rho.$$

It suffices to observe that an augmented system may be written namely the following system satisfied by $(\rho, u, w) = (\rho, u, \nabla \varphi(\rho))$ with $\sqrt{\rho} \varphi'(\rho) = \sqrt{K(\rho)}$:

$$\begin{aligned} \partial_t \rho + \operatorname{div}(\rho u) &= 0, \\ \partial_t(\rho u) + \operatorname{div}(\rho u \otimes u) + \nabla p(\rho) &= \operatorname{div}(F(\rho) \nabla^t w) + \nabla((F'(\rho)\rho - F(\rho)) \operatorname{div} w), \\ \partial_t(\rho w) + \operatorname{div}(\rho w \otimes u) &= -\operatorname{div}(F(\rho) \nabla^t u) - \nabla((F'(\rho)\rho - F(\rho)) \operatorname{div} u) \end{aligned}$$

where $F'(\rho) = \sqrt{K(\rho)\rho}$. Note the skew-symmetric matrix in terms of (u, w) of the right-hand side in the augmented momentum equations. Such formulation may be written if we use the following relation

$$2\rho \nabla(\sqrt{K(\rho)} \Delta(\int_0^\rho \sqrt{K(s)} ds)) = \operatorname{div}(F(\rho) \nabla \nabla \varphi(\rho)) + \nabla((F'(\rho)\rho - F(\rho)) \Delta \varphi(\rho))$$

observed in [8] and which generalizes the Böhm identity. It is interesting to note that the right-hand side may be written as

$$2\operatorname{div}(\mu(\rho) \nabla w) + \nabla(\lambda(\rho) \operatorname{div} w)$$

with $\lambda(\rho) = 2(\mu'(\rho)\rho - \mu(\rho))$ with $\mu(\rho) = F(\rho)/2$.

Mathematics and numerical purposes related to these observations?

Note that the augmented formulation allows to introduce a beautiful notion of relative entropy related to the bi-fluid structure. It is then possible to use the relative entropy method to show several results, as the weak-strong uniqueness, the convergence to a dissipative solution of compressible or incompressible Euler (Euler-Korteweg) equations, and the convergence of the viscous shallow water equations to the inviscid shallow water equations in the vanishing viscosity limit. The interested reader is referred to [7] and [9]. It is also important to note that several global existence of weak solutions for compressible systems with density dependent viscosities has been obtained since the discovering of the structure by

D. Bresch and B. Desjardins: the final version concerning the viscous shallow water introduced at the beginning is due to A. Vasseur and C. Yu published in [13] and J. Li and Z.P. Xin in [12]. Note that a result with the algebraic constraint between $\lambda(\rho)$ and $\mu(\rho)$ will be the subject of a forthcoming paper by D.B. and A. Vasseur and C. Yu. It is also interesting to note that the augmented system for the Euler-Korteweg system allows the authors in [8] to construct a numerical scheme with entropy stability property under a hyperbolic CFL condition in the multi-dimensional setting.

REFERENCES

- [1] H. Brenner. *Navier-Stokes revisited* Phys. A, 349(1-2):60–132, 2005.
- [2] H. Brenner *Fluid mechanics revisited* Phys. A, 370:190–224, 2006.
- [3] D. Bresch, B. Desjardins *Quelques modèles diffusifs capillaires de type Korteweg*, C. R. Acad. Sci. Paris, section mécanique, 332, no. 11 (2004), 881–886.
- [4] D. Bresch, B. Desjardins *Weak solutions via the total energy formulation and their qualitative properties—density dependent viscosities* Soumis dans Handbook of Mathematical Analysis in Mechanics of Viscous Fluids, Eds Y. Giga et A. Novotny (2016).
- [5] D. Bresch, B. Desjardins, E. Zatorska, *Two-velocity hydrodynamics in Fluid Mechanics, Part II. Existence of global κ -entropy solutions to compressible Navier-Stokes system with degenerate viscosities*, J. J. Math. Pures Appl. 104 (2015), 801–836.
- [6] D. Bresch, P. Noble. *Mathematical derivation of viscous shallow-water equations with zero surface tension* Indiana Univ. Journal, vol. 60, (2011), 1137–1269.
- [7] D. Bresch, P. Noble, J.–P. Vila. *Relative entropy for compressible Navier-Stokes equations with density dependent viscosities and applications* To appear in ESAIM Proc (2017).
- [8] D. Bresch, F. Couderc, P. Noble, J.–P. Vila, *A generalization of the quantum Bohm identity: Hyperbolic CFL condition for Euler–Korteweg equations.*, C.R. Acad. Sciences Paris **354** (2016), 39–43.
- [9] D. Bresch, M. Gisclon, I. Violet, *On Navier-Stokes-Korteweg and Euler-Korteweg systems: application to the quantum hydrodynamic*, Submitted (2016).
- [10] E. Feireisl, A. Vasseur. *New perspectives in fluid dynamics: Mathematical analysis of a model proposed by Howard Brenner*, New directions in mathematical fluid mechanics, 153–179, Adv. Math. Fluid Mech., Birkhauser Verlag, Basel, 2010.
- [11] P.G. Gent. *The energetically consistent shallow water equations*. J. Atmos. Sci., 50, 1323–1325.
- [12] J. Li, Z.P. Xin. *Global Existence of Weak Solutions to the Barotropic Compressible Navier-Stokes Flows with Degenerate Viscosities* See arXiv:1504.06826
- [13] A. Vasseur, C. Yu, *Existence of global weak solutions for 3D degenerate compressible Navier–Stokes equations*, Inventiones mathematicae (2016), 1–40.

Data assimilation algorithm for viscous geophysical models

EDRISS TITI

It’s well-known that the long time behavior of dissipative dynamical system is determined by finitely many parameters, such as determining Fourier-modes, nodal values, etc. We take advantage of this observation to design a data assimilation algorithm for recovering the exact reference solution for various viscous geophysical models by employing coarse spatial mesh measurements of the corresponding solution. In particular, we also know the Charney conjecture for the 3D viscous

Planetary Geophysical mode paradigm which states that one can recover the velocity field and the temperature by employing coarse spatial mesh measurements of the temperature alone.

Numerical Methods for ocean General Circulation Models on Unstructured Grids

PETER KORN

The relatively brief history of Numerical Ocean Modeling begins with the appearance of Kirk Bryans seminal 1969 paper [1]. This paper formed the nucleus from which then the family of Bryan-Cox-Semtner models emerged. We briefly review the history of ocean modelling on structured grids¹ that has dominated ocean modelling, before we continue with the description of more recent attempts by several modelling initiatives to formulate ocean dynamics on *unstructured grids*. Unstructured grid ocean models aim for a better representation of the geometry of the ocean basins and opening new perspectives for local grid refinement. These modelling approaches have to developed novel discretization methods for which computational efficiency is an essential design criterion. We focus on a ubiquitous problem of unstructured grid modelling with low-order methods, namely the imbalance of the degrees of freedom of scalar and vector variables. We focus on the triangular C-grid² that appears to be an attractive choice for global ocean modelling but whose utility for the representation of global ocean dynamics has been fundamentally contested. This is due to a computational mode that appears as noise in the divergence of the horizontal velocity field (see [4], [2]), which deteriorates the vertical velocity to an extend that renders the triangular C-grid useless for global ocean dynamics. So far the answers to the triangular C-grid dilemma consisted in either abandoning the triangular cell geometry or the C-staggering. We describe a new discretization of the ocean equations [3] that provides means for controlling the divergence noise on the triangular C-grid in a way that is compatible with the conservation laws, and thereby restores the utility of the triangular C-grid for global ocean modelling. The discretization approach that we are developing here integrates ideas from several discretization methods such as Finite Elements, Finite Volumes and Mimetic Finite Differences. These methods are integrated through the concept of *admissible reconstructions*. Admissible reconstructions are used to establish a weighted weak form of the ocean equations and this gives us on one hand access to the conservation properties and on the other hand a compatible filter of the spurious mode.

¹The notation when a grid is called structured or unstructured is different in different modelling communities. Here we follow the established terminology in atmosphere and ocean sciences.

²Geophysical fluid dynamics uses Arakawas terminology and refers to a staggering with scalars at cell centers and normal velocity components at cell edges as C-grid, while in computational fluid dynamics this is also known as Marker-and-Cell approach due to Harlow and Welch and in the Finite Element literature this is related to the Raviart-Thomas element.

After having stated the full set of discrete ocean equations of an incompressible Boussinesq fluid with a free surface we provide proofs of the conservation properties for volume, tracer content, tracer variance and for the conservation of total energy. Numerical experiments confirm the ability of the new discretization to suppress the computational mode of the triangular C-grid. A global eddy resolving simulation demonstrates that the model is able to reproduce basic features of the global ocean circulation and shows an eddy field that compares well to observational data.

We extend our discretization approach to key ocean subgrid scale closures such as the mesoscale eddy parametrization of Gent-McWilliams and the isoneutral diffusion. A theoretical analysis proves that our new discretization of these subgrid scale operators retains crucial physical properties of the continuous operators such as the invariance of the density field with respect to the isoneutral diffusion or preservation of the tracer variance by the discrete Gent-McWilliams operator.

We conclude with an outlook on ongoing and future work. This comprises the suggestion of new grids that better capture the equator-to-poleward change of the Rossby radius and the attempt to formulate new transport schemes that reduce the spurious numerical induced mixing. We also aim for a numerical analysis of the new discretization that provides convergence results or error estimates for the ocean equations or geophysically relevant subsets of these equations.

REFERENCES

- [1] K. Bryan, A Numerical Method for the Study of the Circulation of the World Ocean, *J. Comp. Phys.* **4** (1969) 347–376
- [2] S. Danilov, Ocean modeling on unstructured meshes, *Ocean Modelling* **69** (2013) 195–210
- [3] P. Korn, Formulation of an Unstructured Grid Model for Global Ocean Dynamics (submitted)
- [4] P. J. Wolfram, O. B. Fringer, Mitigating horizontal divergence "checker-board" oscillations on unstructured triangular C-grids for nonlinear hydrostatic and nonhydrostatic flows, *Ocean Modelling* **69** (2013), 64–78

The role of near-resonance in time-parallel numerical methods

BETH A. WINGATE

(joint work with Adam Peddle, Terry Haut)

Due to power constraints required for creating silicon based computer processors there is an oncoming shift in type of computer architectures. Processor speedups once enjoyed by the scientific community are being replaced by imposed hundreds-of-millions degrees of parallelism, three orders of magnitude more than achieved by today's highest-performing petascale applications[8]. Porting alone is not expected to be successful because the strong-scaling limit, based on parallelization in the spatial dimensions only, is nearly saturated. More specifically, "strong-scaling limit" means that today's methods which rely on spatial domain-decomposition (parallelization-in-space), are close to being optimised for their parallel performance: for a fixed number of grid points if you increase the number of processors,

you spend too much time communicating between the domains and thus time-to-solution increases. If you add more grid points so that you can add more processors, the mathematics of the problem requires you to take a smaller time step, which also increases the time-to-solution, sometimes beyond its scientific usability. The fundamental issue standing in the way of going beyond the strong-scaling limit is embedded in the mathematical structure of the underlying PDEs that govern the physics many of which share the following mathematical form:

$$(1) \quad \frac{\partial \mathbf{u}}{\partial t} + \frac{1}{\epsilon} L(\mathbf{u}) + N(\mathbf{u}, \mathbf{u}) = D(\mathbf{u}), \quad \mathbf{u}(0) = \mathbf{u}_0,$$

where the linear operator L has pure imaginary eigenvalues, the nonlinear term $N(\mathbf{u}, \mathbf{u})$ is of polynomial type, the operator D encodes a form of dissipation, and ϵ is a small non-dimensional parameter. For notational simplicity, we let $\mathbf{u}(t)$ denote the spatial (vector-valued) function $\mathbf{u}(t, \cdot) = (u_1(t, \cdot), u_2(t, \cdot), \dots)$. The operator $\epsilon^{-1}L$ results in time oscillations on an order $\mathcal{O}(\epsilon)$ time scale, and generally necessitates small time steps if standard explicit numerical integrators are used. Even implicit integrators need to use small time steps if accuracy is required.

To take advantage of new degrees of parallelism available with new heterogeneous computer architectures, examining the role of the time domain is essential and therefore considering long time limits of the governing equations in the development of numerical discretizations is important. A great deal of progress has been made on understanding time-parallelism with dissipative stiffness, where slow singular limits are known to exist, and early work on the subject can be found in Gander *et al.*[3] and Dal *et al.*[1]. With oscillatory stiffness, classical ideas of viewing Eq (1) as a fast singular limit as $\epsilon \rightarrow \infty$ have not been as successful. In this talk I introduce some time-parallel ideas that have unfolded in the numerical analysis community over the last 50 years[4] and introduce a new HMM-type[2] parareal[6] method, called Asymptotic Parallel in Time (APinT)[5], general enough for the case when ϵ is finite. I show that under certain regularity constraints we can show the method has superlinear convergence as $\epsilon \rightarrow 0$ and sketch the ideas behind a new proof for superlinear convergence, one that relies on the role of near-resonances inherent in the PDEs, for the case when ϵ is finite[7].

REFERENCES

- [1] G. BAL AND Y. MADAY, *A ? parareal? time discretization for non-linear PDE's with application to the pricing of an American put*, Recent developments in domain decomposition methods, 23 (2009), pp. 189–202.
- [2] B. ENQUIST AND Y.-H. TSAI, *Heterogeneous multiscale methods for stiff ordinary differential equations*, Math. of Comp., 74 (2005), pp. 1707–1742.
- [3] M. J. GANDER AND E. HAIRER, *Nonlinear Convergence Analysis for the Parareal Algorithm*, in Domain Decomposition Methods in Science and Engineering XVII, vol. 60, 2008, pp. 45–56.
- [4] M. J. GANDER, *50 years of time parallel time integration*, in Multiple Shooting and Time Domain Decomposition, T. Carraro, M. Geiger, S. Korkel, and R. Rannacher, eds., Springer-Verlag, 2015.

- [5] T. HAUT AND B. WINGATE, *An asymptotic parallel-in-time method for highly oscillatory pdes*, SIAM Journal of Scientific Computing, 36 (2014), pp. A693–A736. arXiv:1303.6615.
- [6] J. LIONS, Y. MADAY, AND G. TURINICI, *A "parareal" in time discretization of PDEs*, CR Acad. Sci I-Math., 332 (2001), pp. 661–668.
- [7] A. PEDDLE AND T. HAUT AND B. WINGATE, *An asymptotic parallel-in-time method for highly oscillatory pdes with finite frequencies*, In preparation (2016).
- [8] J. SHALF, S. DOSANJH, AND J. MORRISON, *Exascale computing technology challenges*, in VECPAR, J. Palma, ed., Springer-Verlag, 2010, pp. 1–25.

Simulating all-scale atmospheric dynamics on unstructured meshes

PIOTR K. SMOLARKIEWICZ

(joint work with Joanna Szmelter, Feng Xiao)

Historically, atmospheric models across scales were dominated by finite-difference (FD) and spectral-transform methods for spatial discretisation of their governing PDEs. In particular, since the nineteen-sixties, finite-difference methods operating on regular rectangular grids have prevailed in small and mesoscale models for research of cloud processes and orographic flows, with terrain fitted grids mimicked by continuous mappings and horizontal resolution refinement delegated to nested grids. These techniques are still prevailing in computational studies from planetary boundary layer to regional climate [3]. Meteorological interest in unstructured meshing also dates back to the nineteen sixties, in the context of uniform horizontal discretisation for global flows, stifled a decade later by the success of spectral transforms. In the nineteen seventies spherical harmonics approach became the method of choice for global simulations, and combined with two-time-level semi-implicit semi-Lagrangian time stepping it became a marvel of numerical weather prediction at hydrostatic resolutions. However, the progress of distributed computing in the nineteen nineties revealed efficiency limits of the spherical harmonics, and reinvigorated research into compact-stencil discretisations including the unstructured meshing and related finite-volume (FV) integration methods.

Notwithstanding potential benefits of modelling atmospheric flows with unstructured meshes and growing interest in their use, the unstructured-mesh atmospheric models are still relatively new and have not yet achieved the recognition of structured-grid models commonly used in research and operations. An important specificity of the atmospheric dynamics is that it constitutes a relatively small perturbation about dominant hydrostatic geostrophic balance. Preserving this fundamental equilibrium, while accurately resolving the perturbations about it, conditions the design of atmospheric models and subjects their numerical procedures to intricate stability and accuracy requirements. This specificity of atmospheric flows poses new challenges to anisotropic heterogeneous discretisation and flexible mesh adaptivity, largely developed in the engineering community for neutrally stratified non-rotating flows throughout a range of Mach number regimes.

Our recent work [3] consolidates a decade of systematic efforts on generalising proven nonoscillatory forward-in-time finite-difference (NFTFD) semi-implicit

flux-form integrators of all-scale atmospheric PDEs [1] to a corresponding finite-volume (NFTFV) approach for unstructured meshes.¹ The system of generalised all-scale nonhydrostatic PDEs governing evolution of density, ϱ , potential temperature, θ , and flow velocity \mathbf{u} in an idealised (dry, adiabatic and inviscid) atmosphere can be compactly written as

$$(1) \quad \begin{aligned} \frac{\partial \mathcal{G}\varrho}{\partial t} + \nabla \cdot (\mathcal{G}\varrho\mathbf{v}) &= 0, \quad \frac{\partial \mathcal{G}\varrho\theta'}{\partial t} + \nabla \cdot (\mathcal{G}\varrho\mathbf{v}\theta') = -\mathcal{G}\varrho \left(\tilde{\mathbf{G}}^T \mathbf{u} \cdot \nabla \theta_a \right), \\ \frac{\partial \mathcal{G}\varrho\mathbf{u}}{\partial t} + \nabla \cdot (\mathcal{G}\varrho\mathbf{v} \otimes \mathbf{u}) &= \\ &- \mathcal{G}\varrho \left(\Theta \tilde{\mathbf{G}} \nabla \varphi + \mathbf{g} \Upsilon_B \frac{\theta'}{\theta_b} + \mathbf{f} \times (\mathbf{u} - \Upsilon_C \mathbf{u}_a) - \mathcal{M}'(\mathbf{u}, \mathbf{u}_a, \Upsilon_C) \right). \end{aligned}$$

The system (1) encloses the compressible Euler equations under gravity in a rotating reference frame and their two reduced soundproof forms, the pseudo-incompressible and anelastic equations. The distinction between the three forms lies in definitions of the generalised density ϱ and pressure variable φ , together with the corresponding dimensionless coefficients Θ , Υ_B , and Υ_C that depend on various states of the potential temperature [3]. The subscripts b , 0 and a mark, respectively, a horizontally homogeneous and hydrostatically balanced base state, a constant reference value and the balanced ambient state. The primes denote perturbations with respect to the ambient state—e.g., $\theta' = \theta - \theta_a$ —and the perturbation pressure $\varphi \propto (T/\theta)'$ refers to the Exner function. The symbolism of (1) assumes curvilinear coordinate representation, where $\mathcal{G}(\mathbf{x}, t)$ is the square root of the determinant of the metric tensor (viz. the Jacobian), while $\nabla \cdot (..)$ is the scalar product of spatial partial derivatives with a vector, so $d/dt = \partial/\partial t + \mathbf{v} \cdot \nabla$ takes the path velocity $\mathbf{v} = \dot{\mathbf{x}}$ not necessarily equal to the velocity \mathbf{u} . The $\tilde{\mathbf{G}}\nabla\varphi$ symbolises the product of a known matrix of metric coefficients and the vector of partial derivatives, whereas $\tilde{\mathbf{G}}^T$ transforms \mathbf{u} into \mathbf{v} . The term $\mathcal{M}'(\mathbf{u}, \mathbf{u}_a, \Upsilon_C)$ symbolises perturbation of the metric forces [3].

Each of the five PDEs in (1) can be viewed as a generalised transport equation for a scalar variable Ψ ,

$$(2) \quad \frac{\partial G\Psi}{\partial t} + \nabla \cdot (\mathbf{V}\Psi) = G\mathcal{R},$$

where vector field \mathbf{V} (“advecting”) as well as scalar fields G and \mathcal{R} are assumed to be known functions of time and space. A key element of our NFT integrators for (1) is a second-order-accurate FT template for (2)

$$(3) \quad \Psi_{\mathbf{i}}^{n+1} = \mathcal{A}_{\mathbf{i}} \left(\tilde{\Psi}, \mathbf{V}^{n+1/2}, G^n, G^{n+1} \right) + 0.5\delta t \mathcal{R}_{\mathbf{i}}^{n+1} := \hat{\Psi}_{\mathbf{i}} + 0.5\delta t \mathcal{R}_{\mathbf{i}}^{n+1}.$$

Here \mathcal{A} is a shorthand for the NFT transport operator MPDATA [1, 2], $\tilde{\Psi} := \Psi^n + 0.5\delta t \mathcal{R}^n$, \mathbf{i} indexes position on the mesh, δt is a time interval between two

¹One defining aspect of the NFT schemes is a forward-in-time (FT) two-time-level discretisation of the governing conservation laws, relying on a general Lax-Wendroff concept (a.k.a. the Cauchy-Kowalevski procedure) to admit higher-order accuracy in space and time [3].

consecutive time levels n and $n + 1$, and the $\mathbf{V}^{n+1/2}$ is an $\mathcal{O}(\delta t^2)$ estimate of \mathbf{V} at the intermediate time level. In (1) the mass continuity equation is homogeneous, whereas the entropy and momentum equations have nontrivial rhs that generally depend on all model variables. In the FT framework, the latter favours implicit representations of the rhs forcings—as much for the computational stability as for the solution accuracy. Thanks to the homogeneity, the mass continuity can be integrated straightforwardly with (3), not only updating ϱ but also providing cumulative mass fluxes to form advectors for θ' and all components of \mathbf{u} . Given a colocated mesh and the explicit part of the solution $(\hat{\theta}', \hat{\mathbf{u}})$ evaluated with (3), the closed-form expression for the velocity update can be analytically derived [1, 2] as

$$(4) \quad \mathbf{u} = \check{\mathbf{u}} - \mathbf{C}\nabla\varphi, \text{ where } \check{\mathbf{u}} = \mathbf{L}^{-1}\hat{\mathbf{u}}, \text{ and } \mathbf{C} = \mathbf{L}^{-1}0.5\delta t\Theta^*\tilde{\mathbf{G}}.$$

In (4), $\hat{\mathbf{u}}$ is an algebraic modification of $\hat{\mathbf{u}}$ produced by (3), \mathbf{L}^{-1} and \mathbf{C} denote 3×3 matrices of known coefficients, and indices $|_i^{n+1}$ are discarded as there is no ambiguity. Noting that θ' is updated according to $\theta' = \hat{\theta}' - 0.5\delta t(\tilde{\mathbf{G}}^T \mathbf{u} \cdot \nabla\theta_a)$ upon the velocity update, the only lacking element to complete the solution is the pressure perturbation, and this leads to elliptic boundary value problems (BVPs) for φ , derivable by integrating the evolutionary form of the gas law with a consistent semi-implicit NFT template [2, 3].

In [3] we demonstrated the performance of the outlined NFTFV integrators on unstructured meshes across the range of scales from small-scale convective boundary layers, through mesoscale orographic flows, to planetary weather systems (cf. Fig. 1). These results attest to the success of the NFTFV approach in capitalising on the intrinsic strengths of the FV methodology combining the rigorous conservativeness with the adaptability for arbitrary unstructured meshes and the superior computational stability of the nonoscillatory semi-implicit solution procedure while solving for all scales under a single numerical framework.

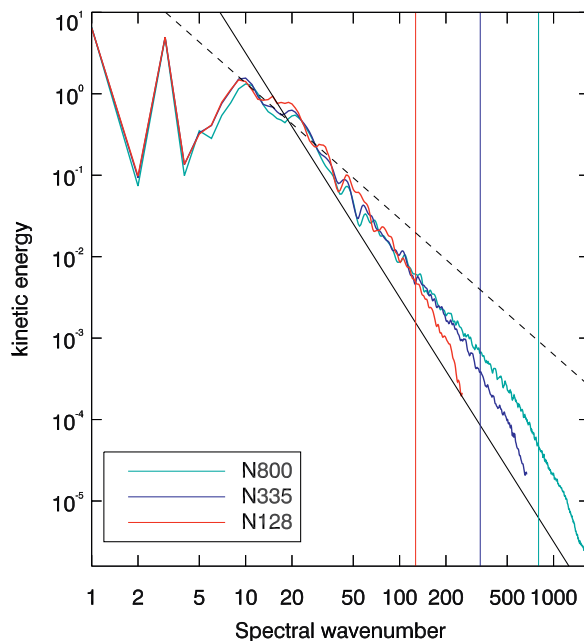


FIGURE 1. Surface kinetic energy spectra at day 9 of the baroclinic instability evolution on the globe, simulated with various horizontal resolutions ($\delta_h \approx 12.5, 30, 78$ km). Vertical lines indicate $4\delta_h$ intervals for each corresponding resolution.

REFERENCES

- [1] P.K. Smolarkiewicz, C. Kühnlein, N.P. Wedi, *A consistent framework for discrete integrations of soundproof and compressible PDEs of atmospheric dynamics*, J. Comput. Phys. **263** (2014) 185–205.
- [2] P.K. Smolarkiewicz, W. Deconinck, M. Hamrud, C. Kuhnlein, G. Mozdzynski, J. Szmelter, N.P. Wedi, *A finite-volume module for simulating global all-scale atmospheric flows*, J. Comput. Phys. **314** (2016), 287–304.
- [3] P.K. Smolarkiewicz, J. Szmelter, F. Xiao, *Simulation of all-scale atmospheric dynamics on unstructured meshes*, J. Comput. Phys. **322** (2016), 267–287.

Causality or correlation? Challenges in data-driven modeling of multiscale geophysical systems

ILLIA HORENKO

One of the challenges in analysis of geophysical systems is to learn about the causality relations in the considered systems on a certain level of resolution - and to distinguish between the true causality from simple statistical correlations. Proper inference of such causality relations, besides giving an additional insight into such processes, can allow improving the respective mathematical and computational models. However, inferring such relations directly from geophysical equations/models is hampered by the multiscale character of the underlying processes and the presence of unresolved/sub-grid scales.

Implications of missing/unresolved scales for this problem will be discussed and an overview of methods for data-driven causality inference will be given. Recently-introduced data-driven multiscale causality inference framework for discrete/Boolean data are explained and illustrated on analysis of historical climate teleconnection series and on inference of their mutual influences on monthly scale.[1]

REFERENCES

- [1] S. Gerber and I. Horenko, *On inference of causality for discrete state models in a multiscale context*, Proceedings of the National Academy of Sciences of USA **111** (2014), 14651-14656.

A Parametrization of Eddy-Mean Flow Interaction based on a Rivlin-Ericksen Stress Tensor

LAURE ZANNA

(joint work with Luca Porta Mana, James Anstey, Tomos David, Thomas Bolton)

Ocean mesoscale eddies are turbulent processes which strongly affect the strength and variability of large-scale ocean jets. Their horizontal scales, roughly 10 to 100 km, are too small to be adequately resolved in current ocean models. Representing eddy-mean flow processes in the current generation of ocean climate remains challenging, especially quantifying the dependence of eddy effects on the underlying dynamics of the resolved flow and external forcing. We present new ways to

diagnose, analyse and parametrize turbulent eddy effects. The work is based on the analysis of idealised and state of the art ocean models, fluid mechanics and stochastic dynamics.

A physically consistent parametrization of eddies, or more precisely of Reynolds stresses, should account for upgradient and downgradient momentum fluxes. It should respect the quasi-geostrophic turbulence properties that there are net up-scale transfers of energy and net downscale transfers of enstrophy, in accordance with the turbulent eddies leading to the production of large-scale jets. The parametrization should also depend on the variability present in the model, as it is intended for use in eddy-permitting models. Our aim is to design a parametrization that incorporates these properties .

Our approach is based on assuming a general stress-deformation relation relying on Rivlin-Ericksen fluid stress tensor series [1, 2]. We assume that turbulent Reynolds stresses can be represented by

$$(1) \quad \frac{D\mathcal{A}}{Dt} + \nabla\mathbf{u}^T\mathcal{A} + \mathcal{A}\nabla\mathbf{u},$$

where $\mathcal{A} = \frac{1}{2}(\nabla\mathbf{u} + \nabla\mathbf{u}^T)$ is the rate of strain. The first term in eq. 1, $\frac{D\mathcal{A}}{Dt}$, is referred to as the memory term, while the last two terms are referred to as the deformation, $\nabla\mathbf{u}^T\mathcal{A} + \mathcal{A}\nabla\mathbf{u}$.

Considering the deformation in a 2D or quasi-2D flow, we can show that the parametrized tendency of turbulent stresses in the momentum equations can be written as

$$\begin{aligned} \frac{\partial u}{\partial t} &= \kappa [(\zeta D)_x - (\zeta \tilde{D})_y] \\ \frac{\partial v}{\partial t} &= -\kappa [(\zeta D)_y + (\zeta \tilde{D})_x] \end{aligned}$$

where $\zeta = v_x - u_y$ is the vorticity, $D = u_y + v_x$ the shearing deformation and $\tilde{D} = u_x - v_y$ the stretching deformation. The parameter κ , with dimension of m^2 , is found to be spatially uniform and to scale with the coarse resolution grid box size. The parametrization is shown to conserve vorticity and energy but also to dissipate enstrophy [5]. The memory term, on the other hand, does not conserve energy and can be interpreted as an energy backscatter, therefore re-introducing lost energy from spurious dissipation [3].

A simplified version of the parametrization has been implemented in a baroclinic quasi-geostrophic model [4]. The parametrization is shown to improve the eddy-mean flow interaction, in a regime in which the largest eddies are resolved. This regime corresponds to the eddy-permitting regime in ocean climate models. In addition, using coarse-graining and conditional probability distribution functions, we can enhance the effect of the parametrization by an introducing a stochastic parametrization which depends on the flow and the forcing. The improvements of the parametrized model versions are shown across a range of model diagnostics and a route towards an implementation in primitive equation is proposed.

REFERENCES

- [1] Rivlin, R. S., Ericksen, J. L., 1955. Stress-deformation relations for isotropic materials. *J. Ration. Mech. Anal.* 4, 323–425.
- [2] Rivlin, R. S., 1957. The relation between the flow of non-Newtonian fluids and turbulent Newtonian fluids. *Q. Appl. Math.* 15, 212–215.
- [3] Porta Mana, P. G. L, Zanna, L., 2014. Toward a stochastic parametrization of ocean mesoscale eddies. *Ocean Modelling.* 79, 1–20.
- [4] Zanna, L., Porta Mana, P. G. L, Anstey J., David T., Bolton T., 2016. Scale-Aware Deterministic and Stochastic Parametrizations of Eddy-Mean Flow Interaction. *Ocean Modelling.* Submitted.
- [5] Anstey J., Zanna, L., 2016. Deformation-based parametrization of mesoscale eddies. *Ocean Modelling.* Submitted.

Different regimes of interactions between scales of motion in the stably stratified atmospheric boundary layer

NIKKI VERCAUTEREN

(joint work with Larry Mahrt, Rupert Klein)

Boundary-layer turbulence in stably stratified weak-wind conditions is typically intermittent and generated partly by shear associated with propagating nonturbulent motions on the so-called submesoscales (corresponding roughly to scales smaller than 2km). These non-turbulent motions can include ramp-cliff patterns, waves or microfronts and are commonly denoted as submesomotions. The diversity of submesomotions complicates the identification of specific physical mechanisms that would potentially trigger intermittent turbulence. In this talk we approach the question of generation of turbulence by submesomotions through statistical clustering combined with in-depth analyses of the dynamical activity of different scales of motions in several datasets of near-surface stable boundary layer turbulence.

The data clustering methodology is a recent method based on a bounded variation, finite element method (FEM-BV) and is used here to characterize the interaction between small-scale non-turbulent motions and turbulence. The clustering methodology achieves a multiscale representation of non-stationary turbulence data by approximating them through an optimal sequence of locally stationary multivariate autoregressive factor models (VARX) processes and some slow hidden process switching between them [1]. The FEM-BV-VARX method is developed by Prof. Illia Horenko at the Università della Svizzera Italiana in Switzerland. We used the FEM-BV-VARX method together with near-surface turbulence data collected over a glacier to objectively separate periods with different influence of the non-turbulent motions on the vertical velocity fluctuations. Regimes were thereby identified, two of them weakly stable and two very stable turbulence states [2]. In each identified regime, we characterized the variability of turbulent momentum fluxes using an extended multiresolution flux decomposition methodology. Transport properties in each regime of near-surface SBL turbulence appear to differ.

Using the same methodology, we investigated the scales of motion responsible for shear generation of turbulence [3].

In turbulence regimes identified in the glacier dataset as little influenced by submesomotions, the multiresolution flux decomposition analysis highlights traditional weakly stable turbulence behavior. In the regimes identified as having a strong influence of submeso forcing, the results suggest a likely direct transfer of energy from the submesoscale horizontal velocity fluctuations to turbulent vertical velocity fluctuations. Those strongly stable regimes are further separated in two clusters that show different dynamics of the scales of motions. Mainly in one of them, the analysis suggests that a scale gap separates submesomotions from turbulence, whereas flux variability is more continuous in scale in the other one without a scale gap. In the latter, the turbulence is probably not in equilibrium with the submesoscale motions because the lack of scale separation implies that the turbulent adjustment time may not be short compared to the time scale of the submesomotions.

REFERENCES

- [1] I. Horenko, *On the Identification of Nonstationary Factor Models and Their Application to Atmospheric Data Analysis*, Journal of the Atmospheric Sciences **67** (5) (2010), 1559–1574.
- [2] N. Vercauteren and R. Klein, *A Clustering Method to Characterize Intermittent Bursts of Turbulence and Interaction with Submesomotions in the Stable Boundary Layer*, Journal of the Atmospheric Sciences **72**(4) (2015), 1504–1517.
- [3] N. Vercauteren, L. Mahrt and R. Klein, *Investigation of interactions between scales of motion in the stable boundary layer*, Quarterly Journal of the Royal Meteorological Society **n/a** (2016), n/a–n/a.

Large deviations in climate dynamics: the examples of abrupt climate changes and extreme heat waves

FREDDY BOUCHET

For some aspects of climate dynamics, rare dynamical events may play a key role. A first class of problems are extreme events that have huge impacts, for instance extreme heat waves. A second class of problems are rare trajectories that suddenly drive the complex dynamical system from one attractor to a completely different one, for instance abrupt climate changes. In the recent past, new theoretical and numerical tools have been developed in the statistical mechanics community, in order to specifically study such rare events. Those approaches are based on large deviation theory for complex dynamical systems. We will present some of these tools and apply them to two paradigmatic examples in climate dynamics. First, the disappearance of one of Jupiter's jets during the period 1939-1940 is a simple example of a drastic climate change related to internal variability. We will demonstrate that quasi geostrophic turbulent models show this kind of ultra rare transitions where turbulent jets suddenly appear or disappear on times scales of tens of thousands times the typical dynamical time scale. We will explain how theoretical and numerical approaches, related to large deviation theory, predict

transition rates, transition paths, and allow to sample transitions in a way that can not be achieved using direct numerical simulations. Second, we will study the probability of extreme heat waves over Europe, in a comprehensive climate model. We will demonstrate that large deviation algorithms allow to sample extremely efficiently extreme heat waves. The thousands of sampled extreme heat waves open the door to their dynamical studies, precursor and fluctuation paths, in a way that can not be foreseen using conventional tools based on model direct numerical simulations.

The Zakharov-L'vov stochastic model for the wave turbulence

SERGEI B. KUKSIN

The wave turbulence (WT) was developed in 1960's to study short scales of small-amplitude solutions for nonlinear PDEs under periodic boundary conditions with long period. The theory applies to hamiltonian PDEs and their perturbations; in particular – to quasi-geostrophic equations (see [6]) and to nonlinear Schrödinger equations (NLS). We start with recalling basic concepts of the theory, using NLS as an example.

1. *Classical setting* (see [2, 3]). Consider the NLS equation

$$\frac{\partial}{\partial t}u + i\Delta u - i\nu |u|^2u = 0, \quad \Delta = (2\pi)^{-2} \sum_{j=1}^d (\partial^2/\partial x_j^2), \quad x \in \mathbb{T}_L^d = \mathbb{R}^d/(L\mathbb{Z}^d),$$

where $d \geq 2$, $L \geq 1$ and $\nu \in (0, 1)$. Denote $H = L_2(\mathbb{T}_L^d; \mathbb{C})$. Then the NLS equation is a hamiltonian system in H with two integrals of motion – the Hamiltonian and the L_2 -norm. I will write solutions u as $u(t, x) \in \mathbb{C}$ or as $u(t) \in H$.

Let us pass to the slow time $\tau = \nu t$ and re-write the equation as

$$(1) \quad \dot{u} + i\nu^{-1}\Delta u - i|u|^2u = 0, \quad \dot{u} = (\partial/\partial\tau)u.$$

We will write the Fourier series for $u(x)$ as

$$(2) \quad u(x) = \sum_{s \in \mathbb{Z}_L^d} v_s e^{2\pi i s \cdot x}, \quad \mathbb{Z}_L^d = L^{-1}\mathbb{Z}^d.$$

Here $\sum_s = L^{-d} \sum_s$, so if $f(x)$ is an integrable continuous function on \mathbb{R}^d , then $\int_{\mathbb{R}^d} f dx \sim \sum_{s \in \mathbb{Z}_L^d} f(s)$ for $L \gg 1$. The objective of the WT is to study solutions of (1) when $\nu \rightarrow 0$, $L \rightarrow \infty$ and $\tau \gg 1$.

2. *Zakharov-L'vov setting*. When studying eq. (1), people from the WT community often talk about “pumping the energy to low modes and dissipating it in high modes”. To make this rigorous, Zakharov-L'vov [1] suggested to consider the NLS equation, dumped by a (hyper)viscosity and driven by a random force:

$$(3) \quad \dot{u} + i\nu^{-1}\Delta u - i\rho |u|^2u = -(-\Delta + 1)^r u + \sum_s b_s \dot{\beta}_s e^{2\pi i s \cdot x}, \quad r > 0.$$

Here ρ is an additional constant, needed later, $\{\beta_s(\tau), s \in \mathbb{Z}_L^d\}$ are standard independent complex Wiener processes¹, the constants $b_s > 0$ fast decay when $|s| \rightarrow \infty$ and are specified below. Solutions $u(\tau)$ of (3) are random processes in the space H . Using in (2), (3) the interaction representation

$$v_s = \exp(i\nu^{-1}\tau|s|^2) a_s, \quad s \in \mathbb{Z}_L^d,$$

we write eq. (3) as

$$(4) \quad \dot{a}_s = -\gamma_s a_s + b_s \dot{\beta}_s + i\rho \sum_{s_1} \sum_{s_2} \delta_{3s}^{12} a_{s_1} a_{s_2} \bar{a}_{s_3} e^{i\nu^{-1}\tau\omega}, \quad s \in \mathbb{Z}_L^d.$$

Here $\gamma_s = (1 + |s|^2)^r$, $\omega = \omega_{3s}^{12} = |s_1|^2 + |s_2|^2 - |s_3|^2 - |s|^2$ and $\delta_{3s}^{12} = 1$ if $s_1 + s_2 = s_3 + s$ and equals zero if otherwise. Note that in view of the factor δ_{3s}^{12} , in the double sum in (4) s_3 is a function of s_1, s_2, s . If $r \geq r(d)$, where $r(d)$ is sufficiently big, then eq. (3) is well posed and mixing. So there is a measure $\mu_{\nu,L}$ in the space H (called *the stationary measure*) such that for any “good” functional F on H and any solution $u(\tau) \in H$ of (3) we have the convergence $\mathbb{E}(F(u(\tau))) \rightarrow \int F(v) \mu_{\nu,L}(dv)$ when $\tau \rightarrow \infty$, see in [4].

The *energy spectrum* of a solution $u(\tau)$ of eq. (3) is the function

$$\mathbb{Z}_L^d \ni s \mapsto n_s(\tau) = n_s^{L,\nu}(\tau) = L^{-d} \mathbb{E}|v_s(\tau)|^2 = L^{-d} \mathbb{E}|a_s(\tau)|^2.$$

3. Discrete turbulence. In order to study the double limit $\nu \rightarrow 0, L \rightarrow \infty$ it is natural to examine first the limit $\nu \rightarrow 0$ (with L fixed), known as the *limit of discrete turbulence*, see [3]. To do this consider the following *effective equation*:

$$(5) \quad \dot{a}_s = -\gamma_s a_s + b_s \dot{\beta}_s + i\rho \sum_{s_1} \sum_{s_2} \delta_{3s}^{12} \delta(\omega) a_{s_1} a_{s_2} \bar{a}_{s_3}, \quad s \in \mathbb{Z}_L^d,$$

where $\delta(\omega)$ is the delta-function of $\omega = \omega_{3s}^{12}$ (equal 1 if $\omega = 0$ and equal 0 otherwise). The following result is proven in [4]. See [7] for its informal description and for discussion of its applications to other equations, including the quasi-geostrophic equation (for the latter also see [6]):

Theorem 1. Eq. (5) is well posed and mixing. When L is fixed and $\nu \rightarrow 0$, then
i) solutions of (4) converge in distribution, on time intervals of order 1, to solutions of (5) with the same initial data at $\tau = 0$;
ii) the measure $\mu_{\nu,L}$ weakly converges to the unique stationary measure of eq. (5).

4. Balance of energy. We provide the space H with the norm $\|\cdot\|$, where

$$\|u\|^2 = L^{-d} \int_{\mathbb{T}_L^d} |u|^2 dx = L^{-d} \sum_s |v_s|^2$$

is the “energy” per unit volume. It is assumed to be of order one, see [2, 3] (so the energy spectrum function n_s also is of order one). Denote $B = L^{-d} \sum_s b_s^2$. Applying the Ito formula to a solution u of (3) we find that

$$(6) \quad \mathbb{E}\|u(\tau)\|^2 + 2\mathbb{E} \int_0^\tau \|(-\Delta + 1)^{r/2} u(s)\|^2 ds = \mathbb{E}\|u(0)\|^2 + 2B\tau.$$

¹i.e. $\beta_s = \beta_s^1 + i\beta_s^2$, where $\{\beta_s^j, s \in \mathbb{Z}_L^d, j = 1, 2\}$ are standard independent real Wiener processes.

Since $\mathbb{E}\|u(\tau)\|^2 \sim 1$ when $L \rightarrow \infty$, we are forced to assume that $B = B(L) \sim 1$. To achieve this, we take any positive continuous function $\tilde{b}(x)$ on \mathbb{R}^d , sufficiently fast decaying at infinity, and set

$$b_s = L^{d/2}\tilde{b}(s), \quad s \in \mathbb{Z}_L^d.$$

Then $B \sim \int \tilde{b}^2 dx \sim 1$ as $L \rightarrow \infty$.

5. *Heuristic result of [5].* Let us choose $\rho = \epsilon L^{1/2}$, where ϵ is a constant of dimension $(\text{length})^{-1/2}$. In [5], arguing on physical level of rigour, we proved the following result, where it is used that since \mathbb{Z}_L^d converges to \mathbb{R}^d as $L \rightarrow \infty$, then asymptotically the energy spectrum $n_s(\tau)$ becomes a function of $s \in \mathbb{R}^d$:

“*Theorem*” 2. Assume that $|\epsilon|$ is sufficiently small. Then under the iterated limit first $\nu \rightarrow 0$, next $L \rightarrow \infty$ the energy spectrum for eq. (3) with properly scaled time, i.e. the function $n_s^{L,\nu}(L^\gamma\tau)$ where γ is a suitable constant, converges to a limiting function $n_s(\tau)$, $s \in \mathbb{R}^d$, satisfying the dump-driven wave kinetic equation

$$(7) \quad \frac{d}{d\tau}n_s(\tau) = -2\gamma_s n_s + \tilde{b}(s)^2 + C_\epsilon \int_{\Gamma_s} \frac{f_s(s_1, s_2, s_3)}{\gamma_s + \gamma_{s_1} + \gamma_{s_2} + \gamma_{s_3}} n_{s_1} n_{s_2} n_{s_3} n_s \\ \times \left(\frac{1}{n_s} + \frac{1}{n_{s_3}} - \frac{1}{n_{s_1}} - \frac{1}{n_{s_2}} \right) ds_1 ds_2 ds_3.$$

Here $\Gamma_s = \{(s_1, s_2, s_3) \in \mathbb{R}^{3d} : s_1 + s_2 = s_3 + s, |s_1|^2 + |s_2|^2 = |s_3|^2 + |s|^2\}$ and the function f_s is defined in terms of the geometry of the surface Γ_s .

Remark. It is also heuristically shown in [5] that the Zakharov ansatz (see [2, 3]) applies to eq. (7) and implies that its time-independent solutions n_s are the Kolmogorov-Zakharov energy spectra [2, 3].

6. *How to make this rigorous?* Unfortunately, we see no way to develop the argument of [5] to a rigorous proof of Theorem 2. Instead, in a work in progress, we establish the following result:

“*Theorem*” 3. Choose $\rho = \epsilon\nu^{-1}$, where $|\epsilon|$ is sufficiently small. Then there exist constants $a_{s_1}, a_{s_2} \in (0, 1)$ such that under the limit

$$L \rightarrow \infty, \quad \nu \rightarrow 0, \quad L^{-a_{s_2}} < \nu < L^{-a_{s_1}},$$

the energy spectrum for eq. (3) with properly scaled time $n_s^{L,\nu}(L^\gamma\tau)$ converges to a limiting function $n_s(\tau)$, $s \in \mathbb{R}^d$, satisfying equation (7).

REFERENCES

- [1] V. Zakharov, V. L’vov, *Statistical description of nonlinear wave fields*, Radiophys. Quan. Electronics **18** (1975), 1084–1097.
- [2] V. Zakharov, V. L’vov, G. Falkovich, *Kolmogorov Spectra of Turbulence*, Springer 1992.
- [3] S. Nazarenko, *Wave Turbulence*, Springer 2011.
- [4] S. Kuksin and A. Maiocchi, *Resonant averaging for small solutions of stochastic NLS equations*, Proceedings A of the Royal Society of Edinburgh, to appear; arXiv:1311.6793v5.
- [5] S. Kuksin, A. Maiocchi, *Derivation of a wave kinetic equation from the resonant-averaged stochastic NLS equation*, Physica D **309** (2015), 65–70.

- [6] S. Kuksin, A. Maiocchi, *The limit of small Rossby numbers for randomly forced quasi-geostrophic equation on β -plane*, *Nonlinearity* **28**, (2015), 2319–2341.
- [7] S. Kuksin, A. Maiocchi, *The effective equation method*, In book “New approaches to Non-linear Waves”, ed. E. Tobisch, Springer 2015.

Variational principles for Stochastic fluid dynamics

DARRYL HOLM

We propose an approach to including stochastic process as “cylindrical noise” in systems of evolutionary PDEs which derive from variational principles that are invariant under a Lie group action. The main objective of the presentation is the inclusion of stochastic processes in ideal fluid dynamics, in which case the variational principle is invariant under “particle relabelling” by smooth invertible maps. Examples include Euler’s fluid equations for incompressible flows and also GFD approximate equations for ocean and atmosphere circular flow. The approach is via a stochastic extension of the Hamilton’s principle for fluid which imposes a constraint of stochastic transport of advected quantities, as obtained from observations of tracers.

Details and examples for GFD may be found in: D.D. Holm, Variational principles for stochastic fluid dynamics, [2015] *Proc Roy Soc A*, 471: 20140963.

Reporter: Jin-Han Xie

Participants

Dr. Ulrich Achatz

FB Geowissenschaften/Geographie
Johann Wolfgang Goethe Universität
Altenhöferallee 1
60438 Frankfurt am Main
GERMANY

Prof. Dr. Gualtiero Badin

Institut für Meereskunde
Universität Hamburg
Bundesstrasse 53
20146 Hamburg
GERMANY

Prof. Dr. Freddy Bouchet

Laboratoire de Physique
ENS - Lyon
46, Allée d'Italie
69364 Lyon Cedex 07
FRANCE

Prof. Dr. Yann Brenier

C M L S
École Polytechnique
Plateau de Palaiseau
91128 Palaiseau Cedex
FRANCE

Prof. Dr. Didier Bresch

Laboratoire de Mathématiques
Université de Savoie
73376 Le Bourget du Lac Cedex
FRANCE

Prof. Dr. Oliver Bühler

Center for Atmosphere Ocean Science
Courant Institute of Mathematical
Sciences
New York University
251, Mercer Street
New York, NY 10012-1110
UNITED STATES

Prof. Dr. Paola Cessi

Scripps Institution for Oceanography
and Physical Oceanography
University of California, San Diego
9500 Gilman Drive
La Jolla CA 92093-0213
UNITED STATES

Dr. Lyuba G. Chumakova

School of Mathematics
University of Edinburgh
James Clerk Maxwell Bldg.
King's Buildings, Mayfield Road
Edinburgh EH9 3JZ
UNITED KINGDOM

Prof. Dr. Mike Cullen

Met Office
Fitzroy Road
Exeter EX1 3PB
UNITED KINGDOM

Prof. Dr. Charles R. Doering

Department of Mathematics
University of Michigan
530 Church Street
Ann Arbor, MI 48109-1043
UNITED STATES

Prof. Dr. Jason E. Frank

Mathematisch Instituut
Universiteit Utrecht
P.O. Box 80.010
3508 TA Utrecht
NETHERLANDS

Prof. Dr. Bernard J. Geurts

Department of Applied Mathematics
University of Twente
P.O.Box 217
7500 AE Enschede
NETHERLANDS

Prof. Dr. Georg A. Gottwald
School of Mathematics and Statistics
The University of Sydney
Sydney NSW 2006
AUSTRALIA

Dr. Ian Grooms
Department of Mathematics
University of Colorado
Boulder, CO 80309-0395
UNITED STATES

Prof. Dr. Peter H. Haynes
Department of Applied Mathematics
and Theoretical Physics (DAMTP)
Centre for Mathematical Sciences
Wilberforce Road
Cambridge CB3 0WA
UNITED KINGDOM

Dr. Sabine Hittmeir
Fakultät für Mathematik
Universität Wien
Oskar-Morgenstern-Platz 1
1090 Wien
AUSTRIA

Prof. Dr. Darryl D. Holm
Department of Mathematics
Imperial College London
Huxley Building
London SW7 2AZ
UNITED KINGDOM

Prof. Dr. Miranda Holmes-Cerfon
Courant Institute of Mathematical
Sciences
New York University
251, Mercer Street
New York, NY 10012-1110
UNITED STATES

Prof. Dr. Illia Horenko
Facoltà di Scienze Informatiche
Università della Svizzera Italiana
Via Giuseppe Buffi 13
6904 Lugano
SWITZERLAND

Prof. Dr. Keith Julien
Department of Applied Mathematics
University of Colorado at Boulder
Campus Box 526
Boulder, CO 80309-0526
UNITED STATES

Prof. Dr. Rupert Klein
FB Mathematik und Informatik
Freie Universität Berlin
Arnimallee 6
14195 Berlin
GERMANY

Dr. Peter Korn
Max Planck Institut für Meteorologie
Universität Hamburg
Bundesstrasse 55
20146 Hamburg
GERMANY

Prof. Dr. Sergei B. Kuksin
Centre de Mathématiques
École Polytechnique
Plateau de Palaiseau
91128 Palaiseau Cedex
FRANCE

Dr. James R. Maddison
School of Mathematics
University of Edinburgh
James Clerk Maxwell Bldg.
King's Buildings, Mayfield Road
Edinburgh EH9 3JZ
UNITED KINGDOM

Prof. Dr. Caroline Muller

Centre de Mathématiques
École Polytechnique
Plateau de Palaiseau
91128 Palaiseau Cedex
FRANCE

Dr. Maxim Nikurashin

Institute for Marine and Antarctic
Studies
University of Tasmania
Private Bag 129
Hobart Tas 7001
AUSTRALIA

Prof. Dr. Marcel Oliver

School of Engineering and Science
Jacobs University Bremen
Campus Ring 1
28759 Bremen
GERMANY

Prof. Dr. Francesco Paparella

Dipartimento di Matematica "E. de
Giorgi"
Università del Salento
CP 193
Via Provinciale Lecce-Arnesano
73100 Lecce
ITALY

Prof. Dr. Olivier Pauluis

Center for Atmosphere Ocean Science
Courant Institute of Mathematical
Sciences
New York University
251, Mercer Street
New York, NY 10012-1110
UNITED STATES

Mark Schlutow

FB Mathematik und Informatik
Freie Universität Berlin
Arnimallee 6
14195 Berlin
GERMANY

Prof. Dr. Shafer Smith

Courant Institute of Mathematical
Sciences
New York University
251, Mercer Street
New York, NY 10012-1110
UNITED STATES

Dr. Piotr Smolarkiewicz

European Center for Medium Range
Weather Forecasts
Shinfield Park
Reading, Berks RG2 9AX
UNITED KINGDOM

Prof. Dr. Samuel N. Stechmann

Department of Mathematics
University of Wisconsin-Madison
480 Lincoln Drive
Madison, WI 53706-1388
UNITED STATES

Jim Thomas

Courant Institute of Mathematical
Sciences
New York University
251, Mercer Street
New York, NY 10012-1110
UNITED STATES

Prof. Dr. Edriss S. Titi

Department of Computer Science
and Applied Mathematics
The Weizmann Institute of Science
Rehovot 76100
ISRAEL

Prof. Dr. Alexandra Tzella

School of Mathematics and Statistics
The University of Birmingham
Edgbaston
Birmingham B15 2TT
UNITED KINGDOM

Prof. Dr. Geoffrey K. Vallis

Department of Mathematics
University of Exeter
North Park Road
Exeter EX4 4QE
UNITED KINGDOM

Dr. Jin-Han Xie

Department of Physics
University of California, Berkeley
376 Le Comte Hall
Berkeley CA 94720-3840
UNITED STATES

Dr. Jacques Vanneste

School of Mathematics
University of Edinburgh
James Clerk Maxwell Bldg.
King's Buildings, Mayfield Road
Edinburgh EH9 3JZ
UNITED KINGDOM

Prof. Dr. William R. Young

Scripps Institution for Oceanography
and Physical Oceanography
University of California, San Diego
9500 Gilman Drive
La Jolla CA 92093-0213
UNITED STATES

Dr. Nikki Vercauteren

FB Mathematik und Informatik
Freie Universität Berlin
Arnimallee 6
14195 Berlin
GERMANY

Prof. Dr. Laure Zanna

Department of Physics and Climate
Physics
University of Oxford
Oxford OX1 3PU
UNITED KINGDOM

Prof. Dr. Xiaoming Wang

Department of Mathematics
Florida State University
Tallahassee, FL 32306-4510
UNITED STATES

Prof. Dr. Vladimir Zeitlin

Laboratoire de Meteorologie Dynamique
École Normale Supérieure
24, rue Lhomond
75231 Paris Cedex 05
FRANCE

Prof. Dr. Beth Wingate

School of Engineering, Computing and
Mathematics (SECaM)
University of Exeter
North Park Road, Harrison Building
Exeter EX4 4QF
UNITED KINGDOM